The Journal of Immunology

RESEARCH ARTICLE | MARCH 24 2023

STAT1 Controls the Functionality of Influenza-Primed CD4 T Cells but Therapeutic STAT4 Engagement Maximizes Their Antiviral Impact FREE

Caroline M. Finn; ... et. al

J Immunol (2023) 210 (9): 1292–1304.
https://doi.org/10.4049/jimmunol.2200407

STAT1 Controls the Functionality of Influenza-Primed CD4 T Cells but Therapeutic STAT4 Engagement Maximizes Their Antiviral Impact

Caroline M. Finn, Kunal Dhume, Emily Prokop, Tara M. Strutt, and K. Kai McKinstry

It is generally accepted that influenza A virus (IAV) infection promotes a Th1-like CD4 T cell response and that this effector program underlies its protective impact. Canonical Th1 polarization requires cytokine-mediated activation of the transcription factors STAT1 and STAT4 that synergize to maximize the induction of the "master regulator" Th1 transcription factor, T-bet. Here, we determine the individual requirements for these transcription factors in directing the Th1 imprint primed by influenza infection in mice by tracking virus-specific wild-type or T-bet-deficient CD4 T cells in which STAT1 or STAT4 is knocked out. We find that STAT1 is required to protect influenza-primed CD4 T cells from NK cell–mediated deletion and for their expression of hallmark Th1 attributes. STAT1 is also required to prevent type I IFN signals from inhibiting the induction of the Th17 master regulator, Rorγt, in Th17-prone T-bet$^{-/-}$ cells responding to IAV. In contrast, STAT4 expression does not appreciably impact the phenotypic or functional attributes of wild-type or T-bet$^{-/-}$ CD4 T cell responses. However, cytokine-mediated STAT4 activation in virus-specific CD4 T cells enhances their Th1 identity in a T-bet-dependent manner, indicating that influenza infection does not promote maximal Th1 induction. Finally, we show that the T-bet-dependent protective capacity of CD4 T cell effectors against IAV is optimized by engaging both STAT1 and STAT4 during Th1 priming, with important implications for vaccine strategies aiming to generate T cell immunity. ***The Journal of Immunology*****, 2023, 210: 1292–1304.**

CD4 T cells protect against influenza A virus (IAV) infection through multiple mechanisms (1, 2). Their importance is seen, for example, through analysis of MHC class II–deficient mice that lack CD4 T cells and that are marked by delayed IAV clearance compared with wild-type (WT) mice (3) and in studies finding that although WT mice depleted of CD8 T cells can clear sublethal IAV infection, mice depleted of both CD4$^+$ and CD8$^+$ cells do not survive (4). Furthermore, IAV-specific effector CD4 T cells isolated from mice during primary infection and transferred to naive hosts can protect against an otherwise lethal IAV challenge (5, 6). Indeed, IAV-specific memory CD4 T cells generated through infection or vaccination are critical components of optimal immunity in mice and humans, especially when preexisting neutralizing Abs are absent (2, 7–9).

To successfully combat pathogens, CD4 T cells must differentiate into specialized effector subsets that are marked by distinct phenotypic and functional attributes (10). This process is initiated by innate cytokines produced upon infection that promote the expression of so-called master regulator transcription factors. Although there is heterogeneity within the pool of IAV-primed CD4 T cells (11), the vast majority express hallmarks of the Th1 subset, an effector program that is strongly associated with protection against IAV (12). These include expression of the Th1 master regulator T-bet, production of the cytokines IFN-γ and TNF, and upregulation of the chemokine receptor CXCR3, which optimizes trafficking of effector cells to the infected lung (13). These and other Th1 attributes are thus widely used to assess CD4 T cell responses in animal and clinical studies focusing on IAV and on viral infection more generally.

We recently showed that T-bet-deficient CD4 T cells still can give rise to effector cells with some Th1 identity during IAV infection (13) and that the transcription factor eomesodermin (Eomes) is essential to promote these residual Th1 attributes (14). Although the regulation of Eomes induction in CD4 T cells is incompletely understood, it has been associated with Th1 programming in some situations (15). This suggests that upstream signaling involved in Th1 induction could be responsible for promoting both T-bet and Eomes expression in CD4 T cells responding to IAV. Interestingly, although very few WT CD4 T cells primed by IAV develop into Th17 cells, some IAV-primed T-bet$^{-/-}$ cells, and even more T-bet$^{-/-}$/Eomes$^{-/-}$ cells, acquire Th17 hallmarks, including expression of the Th17 master regulator, Rorγt, and production of IL-17 and IL-22. This alternative antiviral Th17 programming in CD4 T cells lacking T-bet and Eomes is directed by IL-6 and TGF-β present in the infected lung (14). Whether upstream transcriptional regulators of Th1 differentiation constrain Th17 development in T-bet$^{-/-}$ CD4 T cells is unclear, but it is important to address because highly polarized Th17 effectors can also protect against IAV (14) and are thus a potential target of vaccination.

Division of Immunity and Pathogenesis, Burnett School of Biomedical Sciences, College of Medicine, University of Central Florida, Orlando, FL

ORCIDs: 0000-0001-8843-7773 (E.P.); 0000-0002-4465-1783 (T.M.S.); 0000-0002-5038-7229 (K.K.M.).

Received for publication June 7, 2022. Accepted for publication February 22, 2023.

This work was supported by the National Institutes of Health Grants R21 AI146647 and R01 AI167994 (to K.K.M.) and funds provided by the University of Central Florida (K.K.M. and T.M.S.), by a University of Central Florida Doctoral Support Award (C.M.F.), and by a Solomon Klotz Excellence in Immunology and Allergy Award (C.M.F.). The funders had no role in the design or conduct of the study or in the collection, analysis, or interpretation of data. The funders had no role in the preparation, review, or approval of the manuscript.

Address correspondence and reprint requests to Dr. K. Kai McKinstry, University of Central Florida, 6900 Lake Nona Boulevard, Orlando, FL 32827. E-mail address: kai.mckinstry@ucf.edu

The online version of this article contains supplemental material.

Abbreviations used in this article: dLN, draining lymph node; dpi, days postinfection; Eomes, eomesodermin; IAV, influenza A virus; MHC-I, MHC class I; MFI, mean fluorescence intensity; PA, polymerase; WT, wild type;

STAT1 and STAT4 are critical "pioneering" transcription factors that support the initial phases of Th1 development largely by promoting strong T-bet expression. Activation of STAT1, classically through IFN-γ signaling, initiates T-bet activity that is stabilized and further enhanced through STAT4 activation, classically in response to IL-12 (16). These pathways can act independently to promote degrees of Th1 identity in some settings (17), and STAT4 activation can support certain aspects of Th1 programing independently of T-bet (18–20). The extent to which STAT1 activation can promote Th1 programming in the absence of T-bet is not as clear. Furthermore, the relative degree to which the STAT1 and STAT4 pathways in CD4 T cells responding to IAV regulate the development of antiviral CD4 T cell effectors has not been critically assessed. Here, we delineate the individual requirements for STAT1, STAT4, and T-bet expression by CD4 T cells during IAV infection in promoting Th1 identity and protective capacity in WT CD4 T cells. We also determine how STAT1 and STAT4 regulate the Eomes-dependent Th1 attributes as well as the Th17 attributes that develop in T-bet$^{-/-}$ cells primed by IAV. To do so, we tracked virus-specific WT or T-bet$^{-/-}$ CD4 T cells deficient for either STAT1 or STAT4 during primary IAV infection in otherwise WT mice. This experimental approach focuses on CD4 T cell–intrinsic regulation by STAT1 or STAT4 in the context of a STAT1- and STAT4-replete environment during the infection.

We find that STAT1 expression is required to protect IAV-primed effector cells from NK cell–mediated deletion and for them to express T-bet-dependent phenotypic and functional Th1 hallmarks at levels comparable to WT IAV-primed effector cells. Unexpectedly, STAT1 is also needed for T-bet$^{-/-}$ cells to develop Th17 responses; its expression is required to prevent a type I IFN (IFN-α/β) signaling pathway that restricts Rorγt induction in T-bet$^{-/-}$ CD4 T cells responding in the infected lung. In contrast, STAT4 does not impact the phenotypic or functional attributes of WT or T-bet$^{-/-}$ cells primed by IAV. However, treatment of infected mice with IL-12, which activates STAT4, dramatically enhances the Th1 imprint of WT but not of T-bet$^{-/-}$ cells. Furthermore, priming WT IAV-specific CD4 T cells in vitro with both STAT1- and STAT4-activating cytokines to maximize their Th1 imprint promotes effector cells that are better able to protect naive mice against lethal IAV challenge than STAT1$^{-/-}$ and especially STAT4$^{-/-}$ cells primed in the same conditions. Our findings support the concept that vaccines harnessing STAT4 activation to boost Th1 differentiation beyond that induced naturally by infection could significantly improve T cell immunity against IAV.

Materials and Methods

Mice

Naive donor CD4 T cells for adoptive transfer experiments were obtained from 4–8-wk-old OT-II TcR transgenic mice on either a WT, *Tbx21*$^{-/-}$ (T-bet$^{-/-}$), *Stat4*$^{-/-}$ (STAT4$^{-/-}$), *Stat1*$^{-/-}$ (STAT1$^{-/-}$), *Tbx21*$^{-/-}$*/Stat4*$^{-/-}$ (T/S4$^{-/-}$), or *Tbx21*$^{-/-}$*/Stat1*$^{-/-}$ (T/S1$^{-/-}$) B6 background. The OT-II TcR recognizes aa 323–339 of chicken OVA. WT B6.CD45.1 mice 8–12 wk old were used as hosts for adoptive transfer experiments. In some experiments, mice deficient for expression of IL-12 receptor β-chain (IL-12Rβ$^{-/-}$) were used as hosts. WT, STAT1$^{-/-}$, and STAT4$^{-/-}$ B6 mice not on a transgenic background were infected with IAV in some experiments. All mice were originally obtained from The Jackson Laboratory (Bar Harbor, ME) and bred at the University of Central Florida. Age- and sex-matched groups of B6.CD45.1 mice were purchased as hosts for adoptive transfer experiments and allowed to acclimatize to conditions in the University of Central Florida Lake Nona vivarium for at least 1 wk prior to use. All experimental animal procedures were approved by and conducted in accordance with the University of Central Florida's Animal Care and Use Committee's guidelines.

CD4 T cell isolation, effector cultures, and cell transfer

Naive CD4^{+} cells from unmanipulated OT-II donor mice were obtained from pooled spleen and lymph nodes. Single-cell suspensions were incubated on nylon wool for 1 h followed by Percoll gradient separation to isolate small, resting lymphocytes, and then positive MACS selection using CD4 microbeads (Miltenyi Biotec, Auburn, CA). The resulting cells were routinely >97% TcR^{+} and expressed a naive phenotype (CD62L^{high}, CD44^{low}). Naive CD4 cells were used to generate effector cells in vitro or in adoptive transfer experiments.

Effector cells were generated as previously described (21) using irradiated T-depleted spleen cells as APC and OVA_{II} peptide. All cultures were supplemented with IL-2 at 11 ng/ml. Th1 culture conditions were further supplemented with anti-IL-4 Ab (clone 11B11) at 15 μg/ml and IL-12 at 2 ng/ml. Some cultures were also supplemented with IFN-γ at 1000 U/ml. Th0 cultures were supplemented with anti-IFN-γ Ab (XMG1.2) at 15 μg/ml, anti-IL-4 at 15 μg/ml, and anti-IL-12p40 (C17.8) at 15 μg/ml. Some Th0 cultures were supplemented with IFN-α and IFN-β at 100 U/ml. All blocking Abs were purchased from Bio X Cell (West Lebanon, NH). All other reagents were purchased from PeproTech (Rocky Hill, NJ). Effector cultures were fed with fresh media supplemented with IL-2 after 2 d, and the resulting effector cells were analyzed at day 4. If applicable, effectors were thoroughly washed after 4 d, counted, and resuspended prior to adoptive transfer experiments. Naive or effector CD4 cells were adoptively transferred to host mice under light anesthesia in 200 μl of RPMI media by retro-orbital injection.

Viral infections and in vivo Ab or cytokine treatments

PR8 and PR8-OVA_{II} (H1N1) were grown in the allantoic cavity of embryonated hen eggs from stocks originally provided by P. Doherty. All viral stocks were characterized at the Trudeau Institute (Saranac Lake, NY). Virus was administered to mice under light isoflurane anesthesia intranasally in 50 μl of PBS. Infected mice were monitored daily for infection-induced morbidity, including weight loss, hunched posture, ruffled fur, and reduced movement; mice were euthanized if humane endpoints were reached.

In some experiments, NK cells were depleted in mice receiving donor OT-II cells by treatment with 400 μg anti-NK1.1 Ab in 200 μl of PBS (PK136, Bio X Cell) at −1, 0, 2, 4, 6 d postinfection (dpi) by i.p. injection. In other experiments, mice received 1 μg of IL-12 (BioLegend, San Diego, CA) in 200 μl of PBS by i.p. injection at 2–6 dpi. Control mice received PBS alone. In other experiments, mice were treated i.p. on days 0, 2, 4, and 6 relative to IAV infection with 250 μg of type I IFN receptor blocking Ab (MAR1-5A3, Bio X Cell) or with an isotype control (MOPC-21, Bio X Cell).

Flow cytometry

Single-cell suspensions were washed, resuspended in FACS buffer (PBS plus 0.5% BSA and 0.02% sodium azide), and incubated on ice with 1 μg of anti-FcR (2.4G2) and optimized concentrations of the following fluorochrome-labeled Abs for surface staining: anti-Thy1.1 (OX-7), anti-Thy1.2 (53-2.1), anti-CD4 (RM4.5), anti-CD45.2, anti-CXCR3 (CXCR3-173), anti-Ly-6C (HK1.4), anti-CD11a (M17/4), anti-MHC class I (anti-MHC-I; 8-8-6), and anti-IL-18r (BG/IL18RA).

For intracellular cytokine staining, cells were stimulated for 4 h with 10 ng/ml PMA and 50 ng/ml ionomycin, and 10 μg/ml brefeldin A added after 2 h. Cells were then surface stained and fixed for 20 min in 4% paraformaldehyde followed by permeabilization for 10 min by incubation in 0.1% saponin buffer (PBS plus 1% FBS, 0.1% NaN_3, and 0.1% saponin). The cells were then stained for cytokine by the addition of fluorescently labeled anti-IFN-γ (XMG1.2), anti-TNF (MP6-XT22), anti-IL-2 (JES6-5H4), anti-IL-17 (TC11-18H10.1), anti-IL-10 (JES5-16E3), or anti-IL-22 (IL22JOP) Abs for 20 min.

Detection of transcription factors by flow cytometry was conducted using intranuclear staining buffers and fixation as per the manufacturer's protocols (Thermo Fisher) with fluorescently labeled Abs against T-bet (Ebio4B10), Rorγt (B2D), and Eomes (Dan11mag). To detect phosphorylated STAT proteins (pSTAT), we used a transcription factor phospho buffer kit (BD Biosciences) as per the manufacturer's instructions with an anti-STAT1 pY701 (4a, BD Biosciences) or anti-STAT4 pY693 Ab (38/p-STAT4, BD Biosciences).

All FACS analysis was performed using BD FACSCanto II (BD Biosciences) or Cytoflex (Beckman Coulter) flow cytometers and FlowJo (BD Biosciences) analysis software. All Abs were purchased from BD Biosciences (San Jose, CA), BioLegend (San Diego, CA), or Thermo Fisher (Waltham, MA).

Detection of pulmonary IAV titer

Pulmonary viral titers were determined by quantitation of viral RNA. RNA was prepared from homogenates made from snap-frozen lungs isolated from

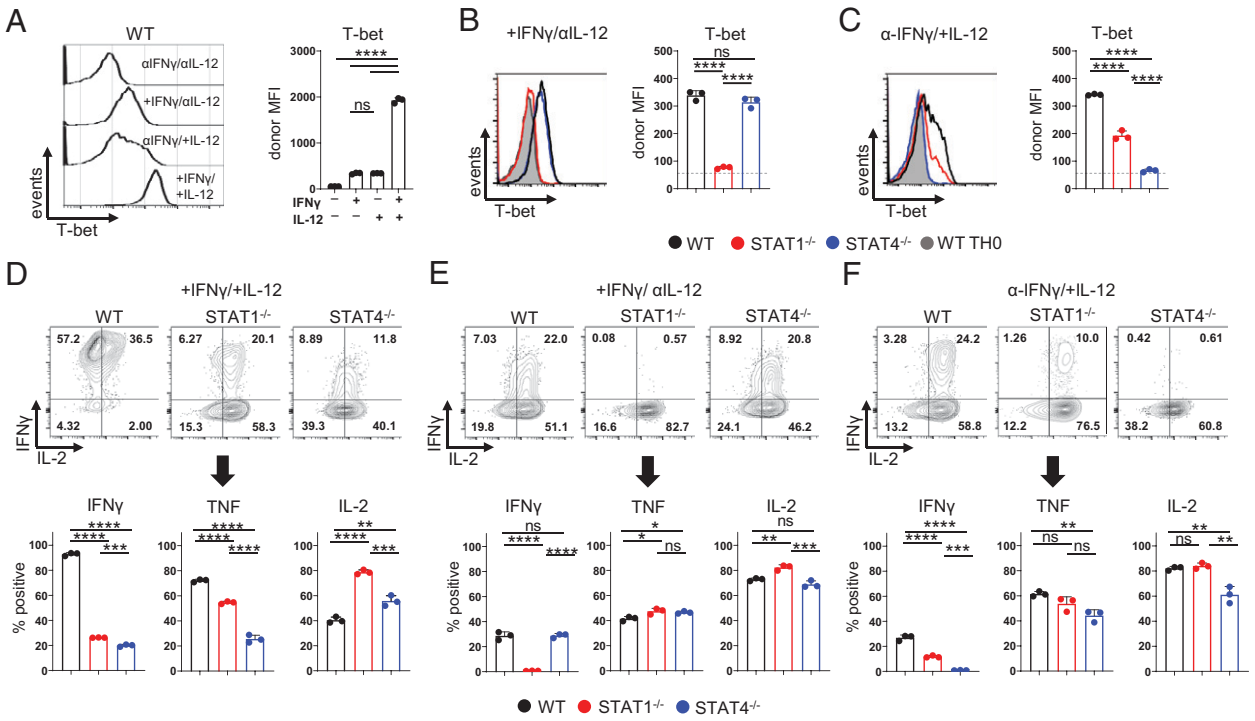

FIGURE 1. STAT1 and STAT4 activating cytokines synergize to promote Th1 differentiation in vitro. Naive WT OT-II cells were cultured with APC and peptide and neutralizing Abs against IFN-γ (αIFN-γ) and IL-12 (αIL-12) (Th0 conditions), with IFN-γ and αIL-12, with IL-12 and αIFN-γ, or with IFN-γ and IL-12 (Th1 conditions). (**A**) After 4 d, effector cells were analyzed for T-bet with representative staining (left) and the MFI from three wells per condition (right). WT, STAT1$^{-/-}$, or STAT4$^{-/-}$ OT-II cells were cultured with WT APC and peptide with (**B**) IFN-γ and αIL-12 or (**C**) IL-12 and αIFN-γ with T-bet expression, including WT Th0 T-bet MFI as a filled gray histogram in representative plots and a dotted line in graphs. Representative staining of IFN-γ and IL-2 production by WT, STAT1$^{-/-}$, and STAT4$^{-/-}$ OT-II cells (top) and summary analysis from three wells for IFN-γ, TNF, and IL-2 production (beneath the arrows) in cultures supplemented with (**D**) IL-12 and IFN-γ, (**E**) IFN-γ and αIL-12, or (**F**) αIFN-γ and IL-12. All results are from one of four independent experiments. $*p < 0.05$, $**p < 0.005$, $***p < 0.001$, $****p < 0.0001$. All error bars represent SD.

infected mice using TRIzol (Thermo Fisher). RNA (2.5 μg) was reverse transcribed into cDNA using random hexamer primers and Superscript II Reverse Transcriptase (Invitrogen). Quantitative PCR was performed to amplify the polymerase (PA) gene of A/PR8-OVA$_{II}$ using a QuantStudio 7 analyzer (Applied Biosystems) with 50 ng of cDNA per reaction and the following primers and probe: forward primer, 5′-CGGTCCAAATTCCTGCTGA-3′; reverse primer, 5′-CATTGGGTTCCTTCCATCCA-3′; probe, 5′-6-FAM-CCAAGTCATGAAGGAGAGGGAATACCGCT-3′. Data were analyzed with Sequence Detector (Applied Biosystems). The copy number of the PA gene per 50 ng of cDNA was calculated using a standard curve made with a PA-containing plasmid of known concentration.

Detection of pulmonary cytokines and chemokines

Levels of cytokines and chemokines in lung homogenates collected as described previously (22) were determined using mouse multiplex kits (EMD Millipore) read on a Bio-Plex Multiplex 200 Luminex reader (Bio-Rad Laboratories) as per the manufacturer's instructions.

Statistical analysis

Unpaired, two-tailed Student *t* tests, $\propto = 0.05$, were used to assess whether the means of two normally distributed groups differed significantly. The Welch correction was applied when variances were found to differ. One-way ANOVA analysis with Bonferroni's multiple comparison posttest was employed to compare multiple means. Significance is indicated as $*p < 0.05$, $**p < 0.005$, $***p < 0.001$, and $****p < 0.0001$. All error bars represent SD.

Results

STAT1 and STAT4 synergize to program Th1 differentiation in vitro

Prior to investigating the transcriptional control of IAV-primed Th1 attributes, we systematically analyzed canonical Th1 development in controlled in vitro settings. We first determined how hallmark STAT1-activating (IFN-γ) and STAT4-activating (IL-12) cytokines impact the induction of T-bet and Eomes during CD4 T cell priming. To do so, we stimulated naive WT OT-II CD4 T cells with APC and cognate peptide for 4 d in Th1 (supplemented with exogenous IFN-γ and IL-12) or Th0 (supplemented with IFN-γ- and IL-12-neutralizing Abs) conditions. Th1 but not Th0 priming promoted strong T-bet induction (Fig. 1A), as expected. The addition to cultures of either IFN-γ or IL-12 alone led to T-bet induction that was approximately five times lower than in full Th1 conditions (Fig. 1A). Eomes induction was also maximal in Th1 cultures and was similar in Th0 cultures and in cells primed with IFN-γ or IL-12 alone (Supplemental Fig. 1). To confirm the dependence of the pro-Th1 actions of IFN-γ and IL-12 on STAT1 and STAT4, respectively, we next compared T-bet and Eomes expression in cultures of WT, STAT1$^{-/-}$, and STAT4$^{-/-}$ OT-II cells. Exogenous IFN-γ promoted T-bet induction in WT and STAT4$^{-/-}$ cells, but not in STAT1$^{-/-}$ cells, when compared with WT Th0 controls (Fig. 1B). Similar patterns of expression were seen for Eomes (Supplemental Fig. 1). IL-12 alone induced T-bet in WT and STAT1$^{-/-}$ cells, but not STAT4$^{-/-}$ cells (Fig. 1C) with little impact on Eomes (Supplemental Fig. 1). IFN-γ and IL-12 signaling, requiring STAT1 and STAT4, respectively, thus synergize to induce maximal expression of T-bet and Eomes during Th1 priming.

We next asked how STAT1 and STAT4 activation impact the production of Th1-associated cytokines. Although more than 90% of WT cells primed in Th1 conditions produced IFN-γ after restimulation, this was reduced approximately fourfold in STAT1$^{-/-}$ and STAT4$^{-/-}$ cells (Fig. 1D). TNF^{+} cells were also maximal in WT Th1 cultures, whereas STAT1$^{-/-}$ and STAT4$^{-/-}$ Th1 cultures contained more IL-2^{+} cells (Fig. 1D). When primed only in the presence of IFN-γ, ~30% of WT and STAT4$^{-/-}$ cells, but virtually no

STAT1$^{-/-}$ cells, were IFN-γ^{+}, whereas TNF^{+} and IL-2^{+} cells were similar across genotypes (Fig. 1E). STAT4$^{-/-}$ cells did not produce IFN-γ when primed with IL-12 alone, whereas ~30% of WT but only ~10% of STAT1$^{-/-}$ cells were IFN-γ^{+} (Fig. 1F). Compromised IFN-γ production by STAT1$^{-/-}$ versus WT cells stimulated with IL-12 is perhaps unexpected and suggests a role for STAT1 in maximizing IL-12-driven IFN-γ production. Supporting this hypothesis, we detected both STAT1 and STAT4 phosphorylation in WT cells cultured in Th0 conditions for 2 d and then stimulated with IL-12 for 20 min (Supplemental Fig. 2), a pattern also reported by others (23). The frequencies of TNF^{+} and IL-2^{+} cells were also lowest in STAT4$^{-/-}$ versus WT and STAT1$^{-/-}$ cells primed with IL-12 alone (Fig. 1F). STAT1 and STAT4 activation thus synergize during Th1 priming to promote IFN-γ and TNF production, with more IL-2 generally seen from effectors with a weaker Th1 imprint, consistent with T-bet's role as a repressor of *Il2* gene transcription (24).

Altered IAV-induced inflammation in STAT1$^{-/-}$ and STAT4$^{-/-}$ mice impacts WT CD4 T cell responses

We next sought to investigate how the STAT1 and STAT4 pathways impact CD4 T cell effectors generated in vivo by IAV infection, which drives a response predominantly characterized by Th1 attributes in WT mice (13). We thus infected WT, STAT1$^{-/-}$, and STAT4$^{-/-}$ mice with a sublethal dose of the mouse-adapted IAV strain, PR8, and analyzed endogenous CD4 T cells in the lungs at 7 dpi. As reported previously (25, 26), numbers of CD44^{high} CD4 T cells were similar between strains (not shown), as were viral titers detected in the lungs at 4 and 7 dpi (Supplemental Fig. 3). However, broad analysis of cytokines and chemokines in lung homogenates at 7 dpi revealed higher levels of 19 of 31 analytes in STAT1$^{-/-}$ versus WT mice, whereas levels of IFN-γ, IL-10, IP-10, MIG, and MIP-1β were reduced in the STAT1$^{-/-}$ mice (Supplemental Fig. 3). The IAV-induced inflammatory environment in STAT4$^{-/-}$ versus WT mice was more similar, but STAT4$^{-/-}$ mice were marked by reduced levels of IFN-γ, IL-10, MIP-1α, and MIP-1β (Supplemental Fig. 3).

We reasoned that the altered inflammatory environments in the IAV-primed STAT$^{-/-}$ mice could impact antiviral CD4 T cell responses independently of CD4 T cell–intrinsic STAT expression status. To test this, we transferred CD90.1^{+} WT OT-II cells to WT, STAT1$^{-/-}$, or STAT4$^{-/-}$ mice and challenged them with PR8-OVA$_{II}$, which is recognized by the OT-II TcR (27). Although WT donor cell numbers in all hosts were similar at 7 dpi, the frequency of IFN-γ^{+} donor cells was reduced in STAT1$^{-/-}$ and STAT4$^{-/-}$ versus WT hosts (Supplemental Fig. 3). The WT donor cells in STAT1$^{-/-}$, but not STAT4$^{-/-}$ or WT, hosts also developed IL-17^{+} cells (Supplemental Fig. 3). Altered inflammatory environments induced by IAV infection as a result of global STAT1 or STAT4 deficiency can thus impact the priming of Th1 and Th17 attributes in WT antiviral CD4 T cells.

CD4-intrinsic STAT1 protects activated cells from NK cell attack and supports a Th1 phenotype

To focus on regulation by CD4 T cell–intrinsic STAT1 and STAT4, we transferred WT or STAT-deficient OT-II cells to congenic WT mice and then challenged the mice with PR8-OVA$_{II}$. We first compared WT and STAT1$^{-/-}$ donor cells at 7 dpi. Strikingly, the recovery of STAT1$^{-/-}$ cells was reduced approximately fivefold in the spleen and draining lymph node (dLN) versus WT cells and ~50 times in the lung, reaching limits of detection (Fig. 2A). Given that STAT1 signaling has been shown to protect proliferating CD4 T cells from NK cell–mediated killing in other in vivo settings (28, 29), we next enumerated STAT1$^{-/-}$ and WT donor cells in host mice treated with NK cell–depleting Ab prior to IAV infection as in our previous studies (30). STAT1$^{-/-}$ donor cells were restored to WT levels in the spleen and dLN by NK cell depletion, but although they were also increased in the lungs, they did not reach WT levels (Fig. 2B). Indeed, when compared with WT donors, the STAT1$^{-/-}$ cells expressed lower levels of MHC-I and of the MHC-I-linked molecule Qa-2 in all organs tested (Fig. 2C), both of which have been associated with protecting CD4 T cells from NK cell attack in vivo (28).

The impaired accumulation of STAT1$^{-/-}$ versus WT effectors in the lungs of NK cell–deficient mice despite similar expansion of both types of donor cells in secondary lymphoid organs mirrors the pattern distinguishing T-bet$^{-/-}$ versus WT CD4 T cell responses against IAV (13). We thus assessed how CD4 T cell–intrinsic STAT1 impacts T-bet expression during IAV infection. We focused on the lungs, the primary site of infection, in NK cell–depleted mice. T-bet was dramatically reduced in STAT1$^{-/-}$ versus WT donor cells. We thus also analyzed T-bet$^{-/-}$ OT-II cells in separate infected NK cell–depleted mice to determine more clearly how STAT1 regulates the expression of T-bet and of T-bet-dependent surface markers expressed by IAV-primed effector CD4 T cells. Using T-bet$^{-/-}$ effector cells as a negative control revealed that most WT cells, but only ~20% of STAT1$^{-/-}$ cells, to be T-bet^{+}, with much lower per-cell T-bet expression in STAT1$^{-/-}$ versus WT cells (Fig. 2D). In contrast, Eomes, which supports the residual Th1 identity of IAV-primed T-bet$^{-/-}$ cells (14), was increased in T-bet$^{-/-}$ cells and even more so in STAT1$^{-/-}$ versus WT cells (Fig. 2E). We found previously that reduced accumulation of T-bet$^{-/-}$ versus WT cells in the lungs correlated with decreased levels of Ly6C, CXCR3, and CD11a on T-bet$^{-/-}$ effectors (13). These markers were all similarly reduced on STAT1$^{-/-}$ and T-bet$^{-/-}$ cells versus on WT cells (Fig. 2F–2H). Together, these results indicate that in addition to protecting IAV-primed CD4 T cells from NK cell–mediated elimination, STAT1 is required for expression of WT levels of T-bet and a T-bet-dependent surface phenotype required for optimal lung homing.

CD4-intrinsic STAT1 is required for maximal Th1 and Th17 function in T-bet$^{-/-}$ CD4 T cells

We next asked how STAT1 impacts Th1 cytokine production by IAV-primed CD4 T cells. Given the similarities between STAT1$^{-/-}$ and T-bet$^{-/-}$ effector phenotypes presented above, and given our previous analysis comparing WT and T-bet$^{-/-}$ effectors (13), we present in Fig. 3 comparisons of STAT1$^{-/-}$ versus T-bet$^{-/-}$ cells, with average values from WT donor cells from the same experiments included as dotted lines. The recipients of all donor cells were depleted of NK cells to normalize the host environment during IAV infection. Infected mice receiving T-bet$^{-/-}$/STAT1$^{-/-}$ (T/S1$^{-/-}$) cells were also included in the same experiments to determine the extent to which STAT1 expression impacts the cytokine production potential of T-bet$^{-/-}$ CD4 T cells. Indeed, in preliminary experiments, we found that IFN-γ production by T/S1$^{-/-}$ cells versus T-bet$^{-/-}$ cells primed in vitro in Th1 conditions was markedly reduced (Fig. 3A), demonstrating robust STAT1-dependent but T-bet-independent priming of Th1 function. Mirroring the pattern seen in STAT1$^{-/-}$ versus WT cells cultured with IL-12, the frequency of IFN-γ^{+} T/S1$^{-/-}$ cells was about half that seen in T-bet$^{-/-}$ cultures (Fig. 3A). This indicates that the requirement for STAT1 in promoting IL-12-dependent IFN-γ production by WT cells (see Fig. 1) is at least partially independent of STAT1-dependent T-bet induction.

The frequency of IFN-γ^{+} cells within the STAT1$^{-/-}$ donor population in IAV-infected lungs was reduced ~30% versus that of T-bet$^{-/-}$ cells and was similar to that of T/S1$^{-/-}$ cells (Fig. 3B).

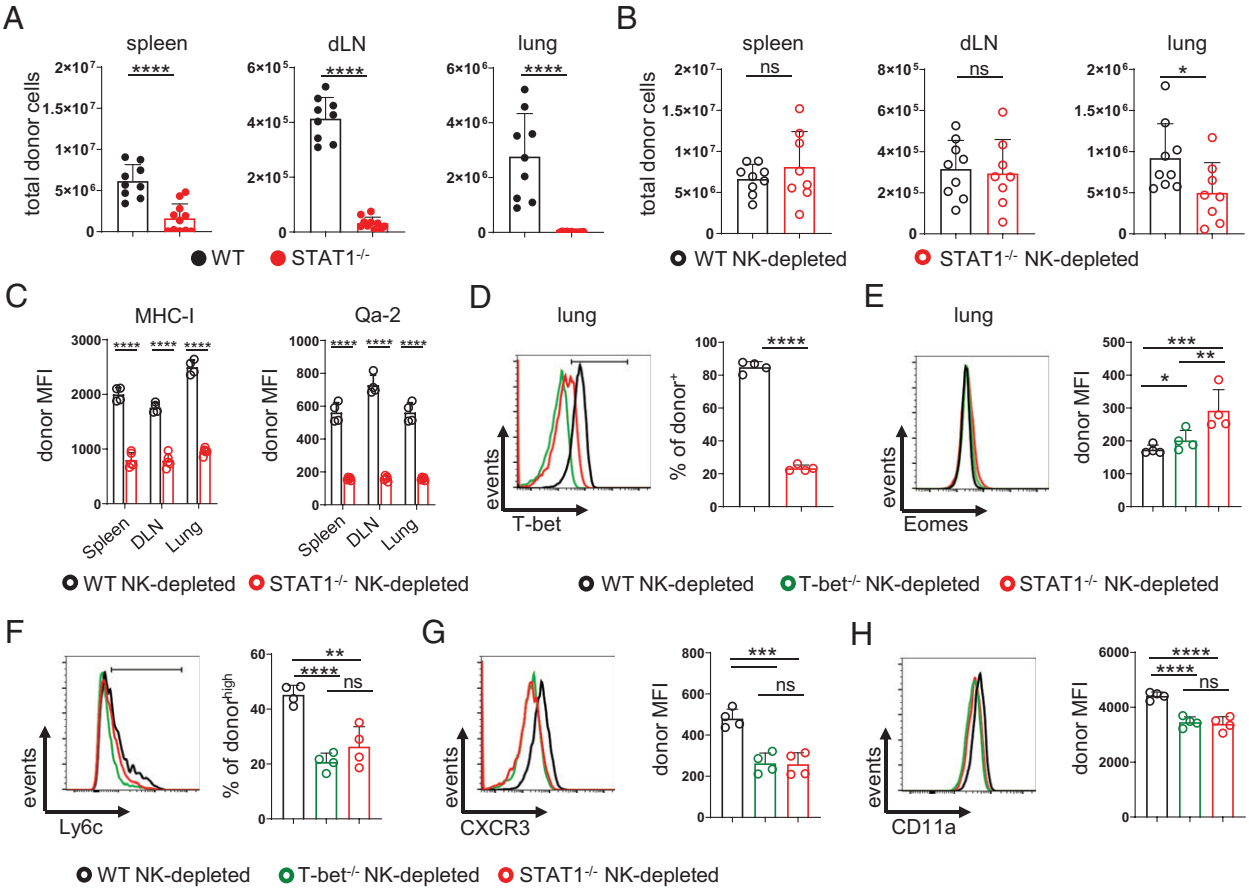

FIGURE 2. STAT1$^{-/-}$ CD4 T cells primed by IAV are susceptible to NK cell attack and lose Th1 identity. Naive WT or STAT1$^{-/-}$ OT-II cells (1×10^6) were transferred to separate congenic WT hosts that were then primed with PR8-OVA$_{II}$. (**A**) Total donor cells in stated organs at 7 dpi. Results from individual mice pooled from two separate experiments. (**B**) Donor cell recovery at 7 dpi from congenic WT hosts that were depleted of NK cells prior to IAV infection. Results pooled from two individual experiments with (**C**) MHC-I and Qa-2 expression by WT and STAT1$^{-/-}$ donor cells responding in separate NK cell–depleted hosts. Results are from one of two experiments. Representative staining of WT, T-bet$^{-/-}$, and STAT1$^{-/-}$ donor cells responding in the lungs of NK cell–depleted hosts at 7 dpi with summary analysis from four mice per group for (**D**) T-bet, (**E**) Eomes, (**F**) Ly6C, (**G**) CXCR3, and (**H**) CD11a. Data for D–G are from one of three similar experiments. *$p < 0.05$, **$p < 0.005$, ***$p < 0.001$, ****$p < 0.0001$. All error bars represent SD.

This is surprising, given the detectable, albeit low, T-bet levels in at least some IAV-primed STAT1$^{-/-}$ cells seen in Fig. 2. TNF production was also reduced in STAT1$^{-/-}$ and T/S1$^{-/-}$ versus in T-bet$^{-/-}$ cells (Fig. 3C). In contrast, IL-2$^+$ cells were increased in STAT1$^{-/-}$ versus T-bet$^{-/-}$ cells and trended higher in T/S1$^{-/-}$ versus T-bet$^{-/-}$ cells (Fig. 3D), consistent with a weaker Th1 functional imprint in cells lacking STAT1 expression. Interestingly, Eomes was increased in STAT1$^{-/-}$ and in T/S1$^{-/-}$ versus in T-bet$^{-/-}$ cells (Fig. 3E). These findings indicate that although Eomes induction in IAV-primed CD4 T cells does not require STAT1, optimal Th1 cytokine production by T-bet$^{-/-}$ cells, which we showed previously requires Eomes (14), is STAT1 dependent.

During IAV infection, autocrine IL-2 production induced by CD4 T cell effectors recognizing viral Ag upregulates their expression of CD127 (IL-7 receptor α-chain), which in turn promotes memory fitness (31, 32). We also found that T-bet$^{-/-}$ effector cells produce more IL-2 and express higher levels of CD127 at 7 dpi with PR8-OVA$_{II}$ than do WT cells, which correlates with improved memory fitness of T-bet$^{-/-}$ versus WT effectors following the resolution of infection (13). However, despite being marked by stronger IL-2 production capacity versus T-bet$^{-/-}$ cells, both STAT1$^{-/-}$ and T/S1$^{-/-}$ cells expressed CD127 only at levels equivalent to WT cells at 7 dpi (Fig. 3F). This suggests that at least some elements of improved memory fitness of T-bet$^{-/-}$ versus WT CD4 T cells primed by IAV may be STAT1 dependent.

IL-10 production during IAV infection is restricted largely to CD4 T cells in the lungs that coproduce high levels of IFN-γ (33). As T-bet expression does not impact IL-10 production by IAV-primed CD4 T cells (13), we tested whether it is impacted by STAT1. Indeed, the frequency of IL-10$^+$ cells was reduced ~80% in STAT1$^{-/-}$ and in T/S1$^{-/-}$ versus in T-bet$^{-/-}$ and in WT cells (Fig. 3G), indicating that IL-10 production is STAT1 dependent but T-bet independent in this setting.

IL-10 signals inhibit Th17 differentiation during IAV infection (33). Furthermore, IAV-primed T-bet$^{-/-}$ cells develop a cohort of Th17 effectors that is not seen during WT CD4 T cell responses (13), consistent with T-bet's restriction of Rorγt-dependent Th17 differentiation (34). Given the impaired expression of both IL-10 and T-bet by STAT1$^{-/-}$ versus WT cells, we hypothesized that STAT1$^{-/-}$ effectors would develop robust Th17 hallmarks. However, neither STAT1$^{-/-}$ nor T/S1$^{-/-}$ donor populations contained many Rorγt$^+$ cells, whereas ~40% of T-bet$^{-/-}$ cells in the same experiments were Rorγt$^+$ (Fig. 3H, 3I). In line with this pattern, few STAT1$^{-/-}$ or T/S1$^{-/-}$ cells produced IL-17 compared with ~15% of T-bet$^{-/-}$ cells that were IL-17$^+$ (Fig. 3J). The STAT1$^{-/-}$ and T/S1$^{-/-}$ cells also did not produce IL-22, whereas T-bet$^{-/-}$ cells did (Fig. 3J). These findings are unexpected because STAT1 activation is strongly associated with the suppression of Th17 development (35–37). Indeed, when plated in Th17-polarizing conditions in vitro, STAT1$^{-/-}$ and T/S1$^{-/-}$ cultures contained more IL-17$^+$ cells than did T-bet$^{-/-}$ cultures (Supplemental Fig. 4). Our

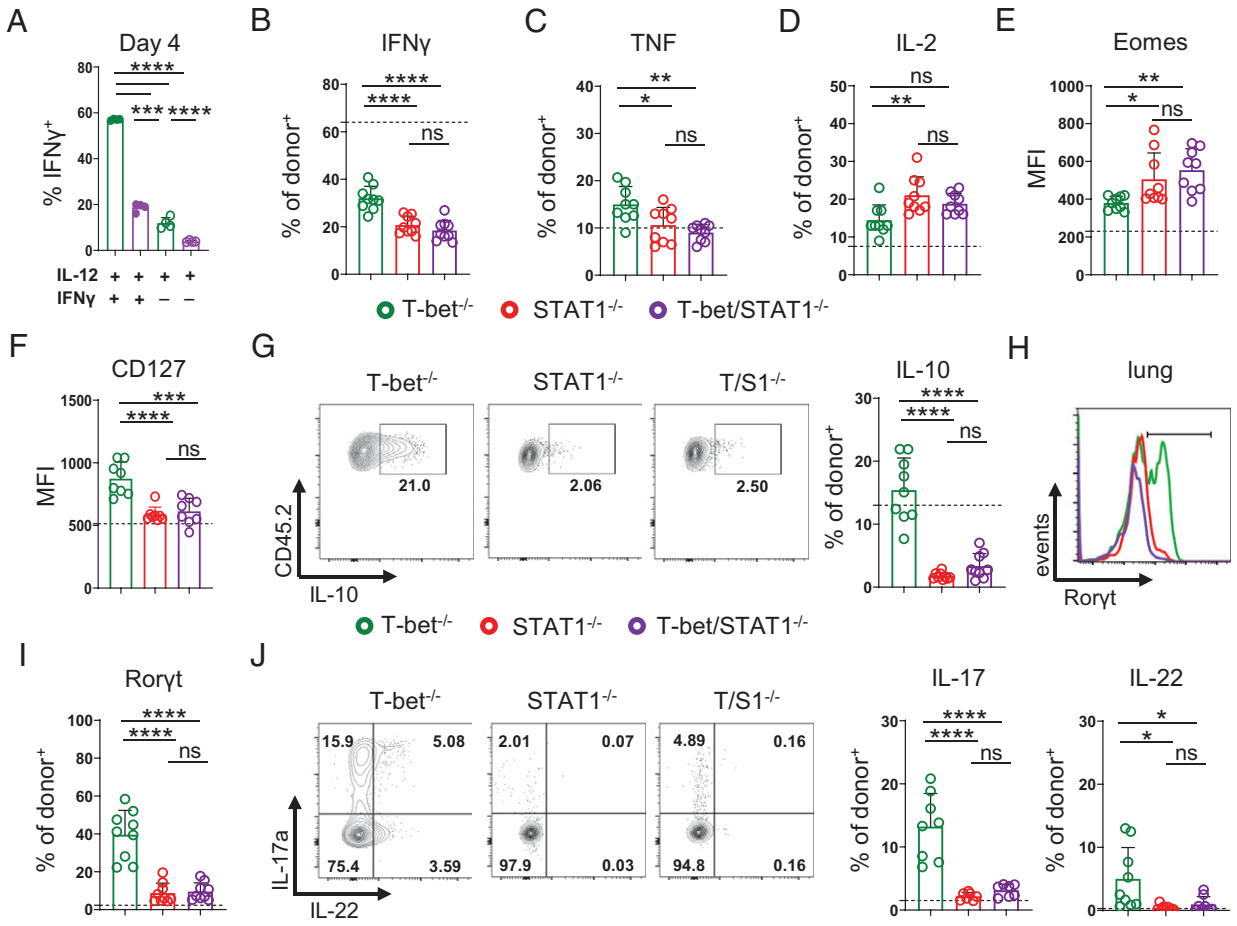

FIGURE 3. STAT1 regulates antiviral function in WT and T-bet$^{-/-}$ CD4 T cells responding to IAV. (**A**) Naive T-bet$^{-/-}$ or T/S1$^{-/-}$ OT-II cells were cultured in triplicate wells with IFN-γ and/or IL-12 as depicted for 4 d. Shown is the frequency of IFN-γ^{+} cells from three wells per condition from one of two experiments. In separate experiments, 1 × 10^{6} T-bet$^{-/-}$, STAT1$^{-/-}$, or T/S1$^{-/-}$ OT-II cells were transferred to congenic NK cell–depleted WT mice that were then primed with PR8-OVA$_{II}$. The frequency of donor cells in the lung at 7 dpi positive for (**B**) IFN-γ, (**C**) TNF, and (**D**) IL-2 is shown from individual mice, as is (**E**) donor cell expression of Eomes and of (**F**) CD127. (**G**) Representative staining and summary analysis of donor cell IL-10 production. (**H**) Representative staining and (**I**) the frequency of Rorγt^{+} donor cells from individual mice. (**J**) Representative staining and the frequency of IL-17- and IL-22-producing donor cells. Results in B–J were pooled from two separate experiments, with dotted lines representing the average value for four WT donor cells responding in separate NK cell–depleted mice. *$p < 0.05$, **$p < 0.005$, ***$p < 0.001$, ****$p < 0.0001$. All error bars represent SD.

results thus reveal, to our knowledge, a novel role for CD4 T cell–intrinsic STAT1 in promoting Th17 responses in vivo during viral infection.

Type I IFN restricts Th17 functionality in IAV-primed STAT1$^{-/-}$ CD4 T cells

The in vitro experiments presented in Supplemental Fig. 4 suggested that STAT1 may not be required for pro-Th17 signaling during IAV infection, but instead could be required to prevent the integration of a signal able to suppress Th17 development. We reasoned that type I IFN could represent such a signal because it has been found to induce IFN-γ production by STAT1$^{-/-}$ but not WT CD8 T cells through a STAT4-dependent mechanism (38, 39). In agreement with these studies, we observed strong STAT4 phosphorylation when Ag-activated STAT1$^{-/-}$ OT-II cells were stimulated with type I IFN in vitro (Fig. 4A). Furthermore, culturing WT, STAT1$^{-/-}$, or STAT4$^{-/-}$ OT-II cells in Th0 conditions supplemented with type I IFN promoted robust IFN-γ production only from STAT1$^{-/-}$ cells (Fig. 4B). This correlated with higher levels of T-bet and Eomes detected in STAT1$^{-/-}$ effectors compared with WT and STAT4$^{-/-}$ cells (Fig. 4C, 4D). Thus, in the absence of CD4 T cell–intrinsic STAT1 expression, direct type I IFN signals can promote strong Th1 polarization in vitro.

Given the results presented above, we reasoned that type I IFN signals received by STAT1$^{-/-}$ cells responding to IAV may support their residual Th1 functionality and suppress Th17 development. To test this, we treated WT mice receiving STAT1$^{-/-}$ OT-II cells with blocking Ab against type I IFN receptor during PR8-OVA$_{II}$ infection. Treatment reduced IFN-γ production by STAT1$^{-/-}$ cells (Fig. 4E), correlating with decreases in T-bet and Eomes expression compared with cells in mice treated with isotype Ab (Fig. 4F). In contrast, an eightfold increase in Rorγt^{+} cells (Fig. 4G) and roughly sixfold increases in IL-17^{+} and IL-22^{+} cells (Fig. 4H) were seen when type I IFN signaling was blocked. These levels of Rorγt and Th17 cytokine production are similar to those seen in T-bet$^{-/-}$ cells (see Fig. 3). Importantly, Th1 cytokine production was similar in CD44^{high} WT host CD4 T cells in the lungs of mice treated with type I IFN receptor blocking or control Ab, with very few Th17 cytokine-producing cells seen, regardless of treatment (Fig. 4I). These results indicate a specific impact of type I IFN in promoting Th1 and repressing Th17 development by STAT1$^{-/-}$ CD4 T cells during IAV infection.

STAT4 is dispensable for IAV-primed Th1 identity in WT and T-bet$^{-/-}$ CD4 T cells

We next compared WT and STAT4$^{-/-}$ donor cells responding in separate IAV-primed WT mice. Numbers of WT and STAT4$^{-/-}$ cells in the infected lungs at 7 dpi were similar (Fig. 5A), as was their expression of the T-bet-dependent surface markers CXCR3,

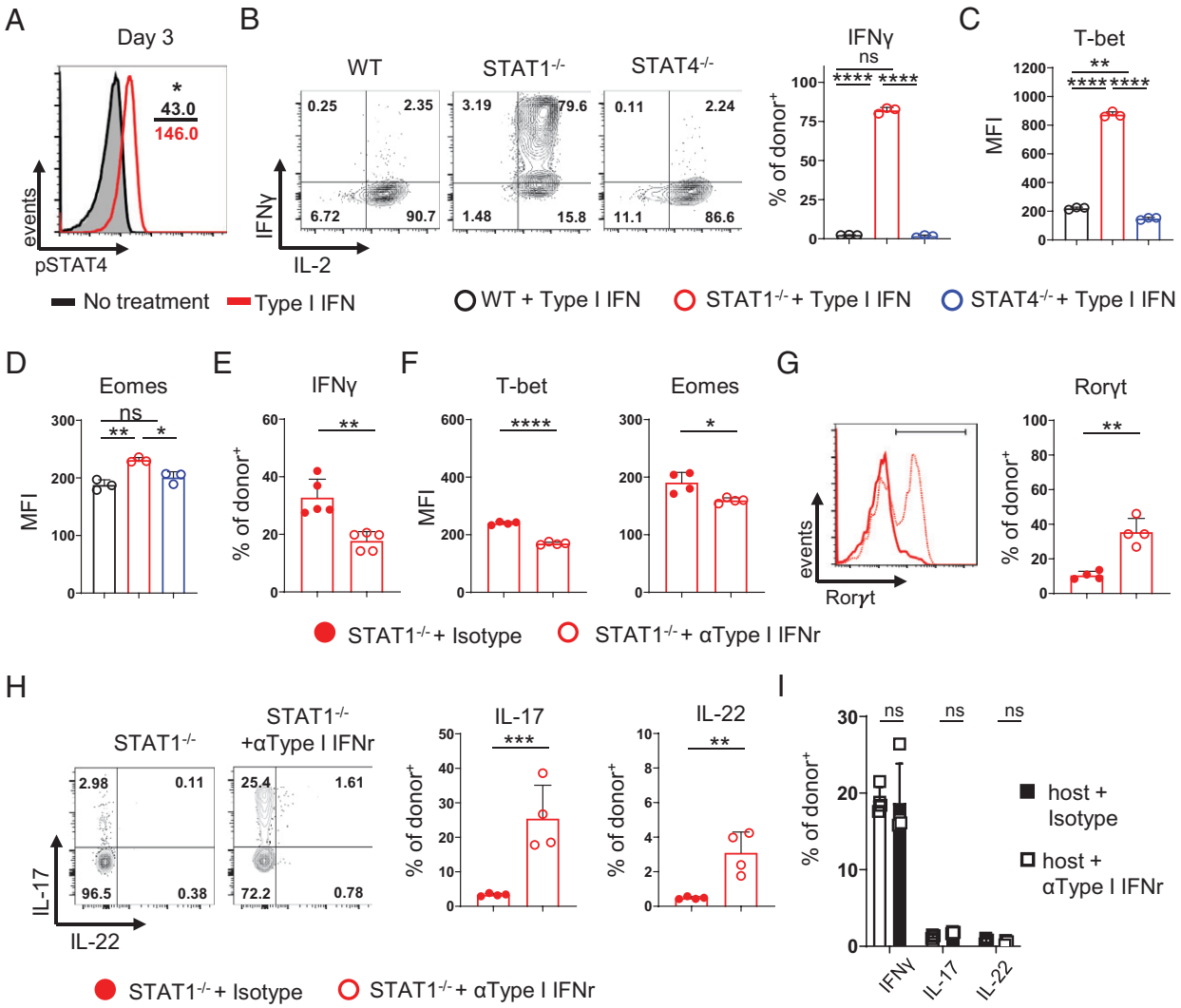

FIGURE 4. Type I IFN signals promote Th1 and inhibit Th17 differentiation in STAT1$^{-/-}$ CD4 T cells during IAV infection. (**A**) Naive STAT1$^{-/-}$ OT-II cells were activated in Th0 conditions for 3 d, then stimulated with type I IFN or not for 20 min and analyzed for pSTAT4. Representative staining, including control staining from STAT4$^{-/-}$ cells primed and treated in the same conditions (filled gray) with the average pSTAT4 MFI from four wells per condition (inset). (**B**) WT, STAT1$^{-/-}$, or STAT4$^{-/-}$ OT-II cells were stimulated in Th0 conditions with type I IFN for 4 d. Representative staining for IFN-γ and IL-2 and summary analysis of IFN-γ production from three wells per condition as well as (**C**) T-bet and (**D**) Eomes expression. All results are from one of three experiments. STAT1$^{-/-}$ OT-II cells were transferred to NK cell–depleted WT host mice that were primed with PR8-OVA$_{II}$ and treated with control or type I IFN receptor blocking Ab (αType I IFNr). (**E**) At 7 dpi, donor cells from individual mice were assessed for IFN-γ production, (**F**) T-bet (left) and Eomes (right), and (**G**) Rorγt and (**H**) production of IL-17 and IL-22. (**I**) Production of stated cytokines by host CD4^{+} CD44^{high} T cells in the lungs of the same mice. All results are from one of at least two independent experiments. *$p < 0.05$, **$p < 0.005$, ***$p < 0.001$, ****$p < 0.0001$. All error bars represent SD.

Ly6C, and CD11a (not shown). T-bet itself, however, was slightly reduced in STAT4$^{-/-}$ cells (Fig. 5B), whereas Eomes was not impacted (Fig. 5C). Despite their marginally reduced expression of T-bet, production of IFN-γ, TNF, and IL-2 by STAT4$^{-/-}$ and WT cells was comparable (Fig. 5D), as was their expression of CD127 (Fig. 5E). Finally, IL-10^{+} cells were similar between WT and STAT4$^{-/-}$ cells, with very few Rorγt^{+}, IL-17^{+}, or IL-22^{+} cells detected in either population (not shown). Thus, in contrast to STAT1's critical regulatory roles, CD4 T cell–intrinsic STAT4 is not required to prime the phenotypic and functional Th1 hallmarks of WT effector cells responding to IAV.

We reasoned that the high levels of T-bet seen in WT and STAT4$^{-/-}$ CD4 T cells could negate requirements for the STAT4 pathway in regulating IAV-driven effector development, but that STAT4 could play a more prominent role in promoting Th1 functionality in T-bet$^{-/-}$ cells. To test the validity of this concept, we generated T-bet$^{-/-}$/STAT4$^{-/-}$ (T/S4$^{-/-}$) mice and first cultured naive T-bet$^{-/-}$ or T/S4$^{-/-}$ OT-II cells in vitro in Th1 conditions. IFN-γ production was dramatically reduced in T/S4$^{-/-}$ versus T-bet$^{-/-}$ cultures (Fig. 5F), confirming robust STAT4-dependent, T-bet-independent Th1 functionality. In contrast, numbers of T-bet$^{-/-}$ and T/S4$^{-/-}$ donor cells responding to IAV in WT mice (Fig. 5G), as well as their production of IFN-γ, TNF, IL-2 (Fig. 5H), and IL-10 (Fig. 5I), was similar. We reasoned that STAT4 activation could antagonize IL-17 production by T-bet$^{-/-}$ cells or, alternatively, that it may be required for it, given STAT4's role in Th17 priming under some conditions (18). However, T-bet$^{-/-}$ and T/S4$^{-/-}$ donors were marked by similar frequencies of IL-17^{+} (Fig. 5J) and IL-22^{+} cells (not shown). Finally, in contrast to the impaired CD127 upregulation by T-bet$^{-/-}$ cells deficient for STAT1, levels of CD127 on T/S4$^{-/-}$ and T-bet$^{-/-}$ effector cells were similar (Fig. 5K). Together these results indicate that the STAT4 pathway does not play a major role in promoting functional or phenotypic attributes of WT or T-bet$^{-/-}$ effectors primed by IAV.

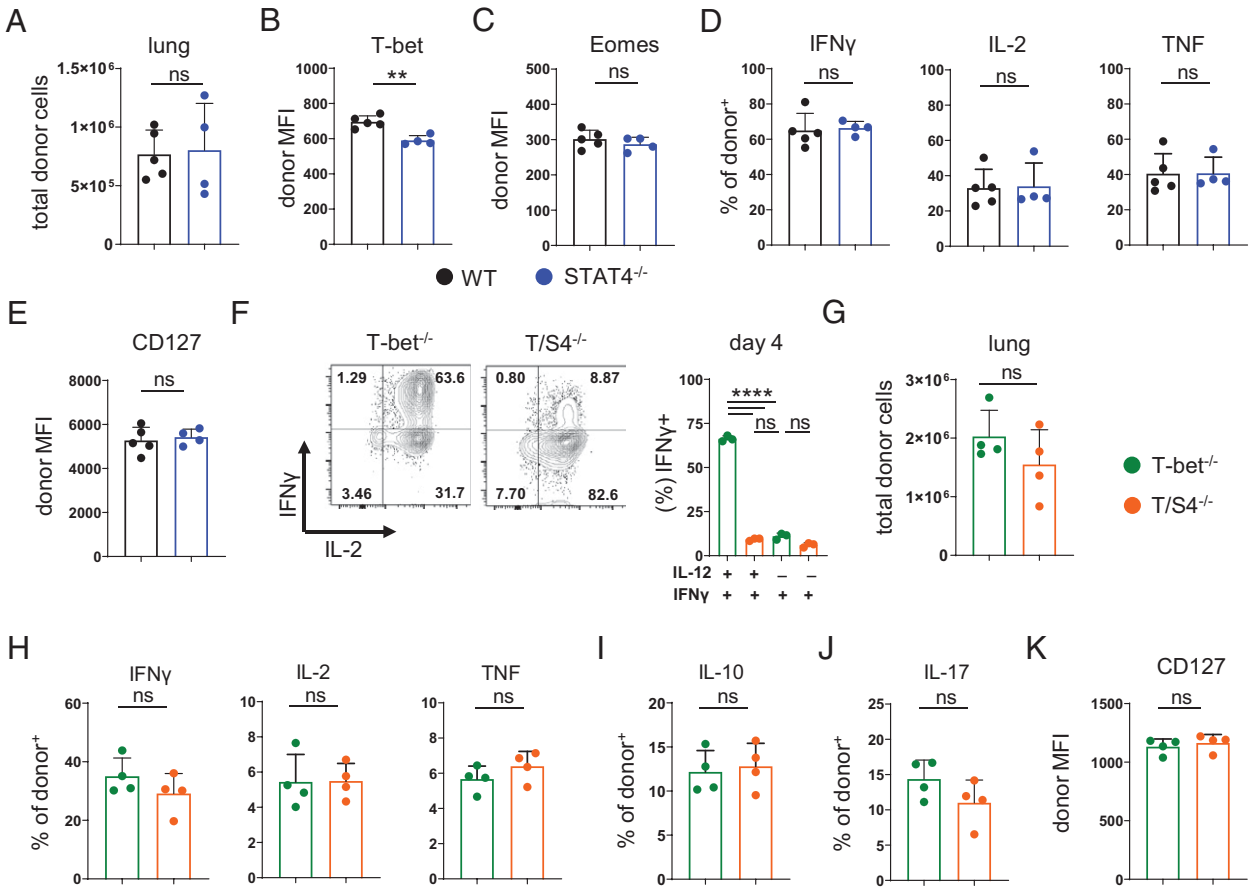

FIGURE 5. CD4-intrinsic STAT4 does not impact the Th1 identity of IAV-primed cells. Naive WT or STAT4$^{-/-}$ OT-II cells (1×10^6) were transferred to congenic WT hosts that were challenged with PR8-OVA$_{II}$. (**A**) The number of donor cells in the lungs at 7 dpi, their MFI of (**B**) T-bet and (**C**) Eomes expression, (**D**) the frequency of IFN-γ$^+$, IL-2$^+$, and TNF$^+$ donor cells after restimulation, and (**E**) their MFI of CD127 expression. (**F**) Naive T-bet$^{-/-}$ or T/S4$^{-/-}$ OT-II cells were cultured with IFN-γ and IL-12 for 4 d with representative staining of IFN-γ and IL-2 production after restimulation and summary for IFN-γ$^+$ cells from individual wells plated in the stated conditions. Results are from one of two independent experiments. In separate experiments, 1×10^6 T-bet$^{-/-}$ or T/S4$^{-/-}$ OT-II cells were transferred to separate congenic hosts and were analyzed at 7 dpi with PR8-OVA$_{II}$. (**G**) The number of donor cells in the lungs, (**H**) their production of IFN-γ, TNF, and IL-2, (**I**) IL-10 and (**J**) IL-17, and (**K**) their expression of CD127. Results are representative of individual mice from one of three experiments. $^{**}p < 0.005$, $^{****}p < 0.0001$. All error bars represent SD.

STAT4 activation by IL-12 enhances the Th1 identity of IAV-primed CD4 T cells

The stark differences between the Th1 imprints of STAT4$^{-/-}$ and WT effectors primed in vitro under Th1 conditions seen in Fig. 1 versus their similarity during IAV infection seen in Fig. 5 suggests that WT cells may not be able to engage STAT4 in the latter setting. To test this, we treated mice receiving WT or STAT4$^{-/-}$ OT-II cells with IL-12 or with PBS alone by i.p. injection from 2 to 6 dpi and analyzed the donor cells at 7 dpi. We first assessed expression of a subunit of the IL-18 receptor (CD218a) known to be upregulated in a STAT4-dependent manner (40). The mean fluorescence intensity (MFI) of CD218a was increased approximately threefold on WT but not STAT4$^{-/-}$ donor cells by IL-12 treatment (Fig. 6A), validating robust STAT4 engagement. T-bet expression by WT cells, but not STAT4$^{-/-}$ cells, was also markedly increased by IL-12 treatment (Fig. 6B). Surprisingly, although most WT CD4 T cells in the lung are T-bet$^+$ (6), using donor cells from the IL-12-treated mice to set a gate revealed only ~20% of WT cells to be T-bet^{high} in control mice. The expression of Eomes by WT but not STAT4$^{-/-}$ cells was also increased by IL-12 treatment (Fig. 6C), consistent with our in vitro findings of synergy between STAT1 and STAT4 activation in promoting Eomes induction. Functionally, IL-12 treatment nearly doubled the frequency of IFN-γ$^+$ WT cells (Fig. 6D) and increased the MFI of the IFN-γ$^+$ cells approximately threefold, indicating enhanced per-cell production (Fig. 6E). Unexpectedly, IL-12 treatment also increased the frequency of IFN-γ$^+$ STAT4$^{-/-}$ donor cells, though to a lesser extent, but it did not impact the MFI of the IFN-γ$^+$ cells.

We next treated recipients of T-bet$^{-/-}$ or T/S4$^{-/-}$ cells with IL-12 to determine the extent to which the STAT4-dependent pro-Th1 impacts of IL-12 are due to increased T-bet expression as seen in Fig. 6B. IL-12 treatment marginally increased IL-18 receptor expression on T-bet$^{-/-}$ but not on T/S4$^{-/-}$ cells (Fig. 6F). Given the threefold increase in MFI of WT cells treated with IL-12 in Fig. 5A, this indicates that T-bet is required for maximal STAT4-dependent upregulation of IL-18 receptor. In further contrast to WT cells, production of IFN-γ by T-bet$^{-/-}$ and T/S4$^{-/-}$ cells was not increased by IL-12 treatment (Fig. 6G). The MFI of the IFN-γ$^+$ T-bet$^{-/-}$ cells was increased slightly, however, whereas that of T/S4$^{-/-}$ IFN-γ$^+$ cells was decreased by IL-12 treatment (Fig. 6H). These results indicate that the pro-Th1 impact of STAT4 activation in CD4 T cells by IL-12 is primarily T-bet dependent.

Elevated systemic production of IFN-γ and/or other proinflammatory impacts of in vivo IL-12 administration in mice seen using similar IL-12 treatment regimens (41) could be required in addition to CD4 T cell-intrinsic STAT4 activation for some or all of the elements of boosted Th1 identity seen above. To test this, we transferred WT OT-II cells to mice deficient for IL-12 receptor

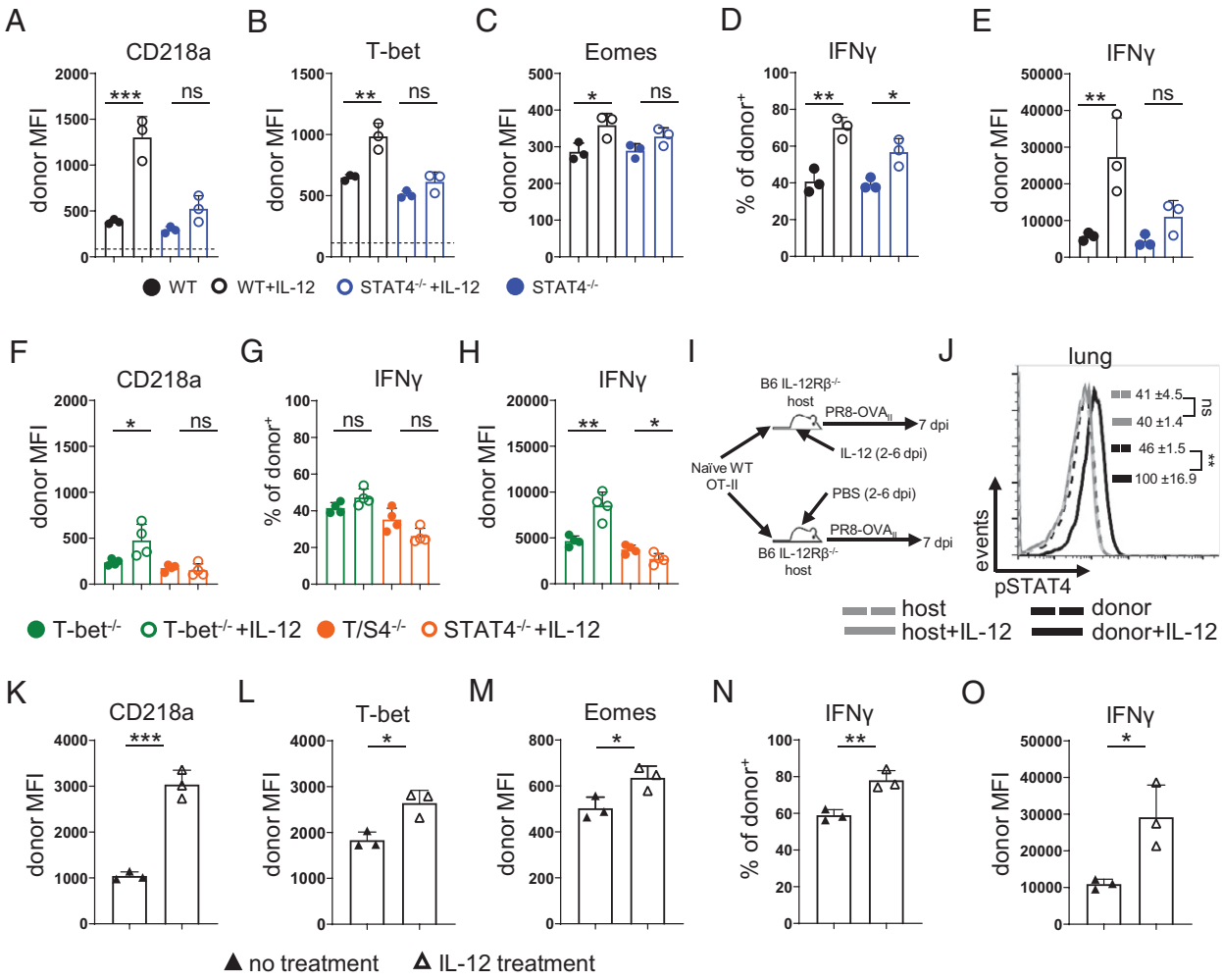

FIGURE 6. STAT4-dependent IL-12 signals can enhance Th1 identity during IAV infection. WT or STAT4$^{-/-}$ OT-II cells were transferred to congenic WT hosts that were then challenged with PR8-OVA$_{II}$. Groups of mice were treated i.p. with IL-12 or PBS alone. (**A**) MFI of CD218a (**B**) T-bet and (**C**) Eomes expression by lung donor cells at 7 dpi, (**D**) the frequency of donor cells producing IFN-γ and (**E**) the MFI of IFN-γ$^+$ cells. Results are from individual mice from one of three experiments. WT host mice received T-bet$^{-/-}$ or T/S4$^{-/-}$ donor cells and were treated with PBS or IL-12. Shown is donor cell (**F**) CD218a expression and (**G**) the frequency of and (**H**) MFI of IFN-γ$^+$ cells. Results are from one of two independent experiments. (**I**) WT OT-II cells were transferred to IL-12Rβ$^{-/-}$ host mice that were infected with PR8-OVA$_{II}$ and treated with PBS or IL-12. (**J**) Representative pSTAT4 staining of host CD44^{high} CD4 T cells and donor cells in the lungs at 7 dpi, with summary MFI analysis from three mice per group (inset), (**K**) the MFI of donor cell CD218a, (**L**) T-bet, (**M**) Eomes, and (**N**) the frequency and (**O**) MFI of IFN-γ$^+$ cells. Results are from one of two experiments. *$p < 0.05$, **$p < 0.005$, ***$p < 0.001$. All error bars represent SD.

β (IL-12Rβ$^{-/-}$), infected the mice with IAV, and treated them with IL-12 or PBS alone (Fig. 6I). pSTAT4 analysis at 7 dpi revealed increased STAT4 phosphorylation in donor, but not host, T cells in mice treated with IL-12 (Fig. 6J), as expected. Importantly, IL-12 treatment increased WT donor cell expression of IL-18 receptor (Fig. 6K), T-bet (Fig. 6L), and Eomes (Fig. 6M), as well as the frequency (Fig. 6N) and MFI (Fig. 6O) of IFN-γ$^+$ cells. Together, these results demonstrate that IAV induces a submaximal Th1 imprint that can be markedly enhanced by therapeutic CD4 T cell–intrinsic STAT4 activation.

Combined STAT1 and STAT4 activation improves Th1-primed CD4 T cell protection against IAV

The results above suggest that synergy between STAT1 and STAT4 activation in CD4 T cells to strengthen their Th1 imprint may improve their protective efficacy against IAV. To test this, we primed naive WT, STAT1$^{-/-}$, or STAT4$^{-/-}$ OT-II cells with APC and peptide in the presence of IFN-γ and IL-12 as in Fig. 1. We then gave 3×10^6 of the resulting effectors to naive WT mice and challenged them with 2 LD$_{50}$ PR8-OVA$_{II}$. This number of WT Th1 effectors transfers robust protection to unprimed mice against otherwise lethal doses of PR8-OVA$_{II}$ (13). Because STAT1$^{-/-}$ CD4 T cells are eliminated by NK cells in WT mice during IAV infection (see Fig. 2), we depleted NK cells in all groups of mice prior to effector transfer to normalize host environments during IAV infection.

We first assessed the Th1 attributes of the effector cells in the lungs at 4 dpi, the peak of their response after transfer in this model (42). STAT1$^{-/-}$ cells expressed less Ly6C than WT or STAT4$^{-/-}$ effectors (Fig. 7A), consistent with its regulation by STAT1, as seen in Fig. 5, whereas STAT4$^{-/-}$ effectors expressed less IL-18 receptor than WT or STAT1$^{-/-}$ effectors, consistent with its regulation by STAT4, as seen in Fig. 6 (Fig. 7B). Furthermore, WT cells expressed more T-bet than either STAT$^{-/-}$ population, consistent with expression patterns prior to transfer, as seen in Fig. 1 (Fig. 7C). WT effectors also produced more IFN-γ (Fig. 7D, 7E) and TNF (Fig. 7F) than STAT1$^{-/-}$ and especially STAT4$^{-/-}$ cells. In contrast, the STAT1$^{-/-}$ and STAT4$^{-/-}$ cells produced more IL-2 (Fig. 7G), consistent with a weaker functional Th1 imprint. Th17 cytokines were not detected from any population (not shown).

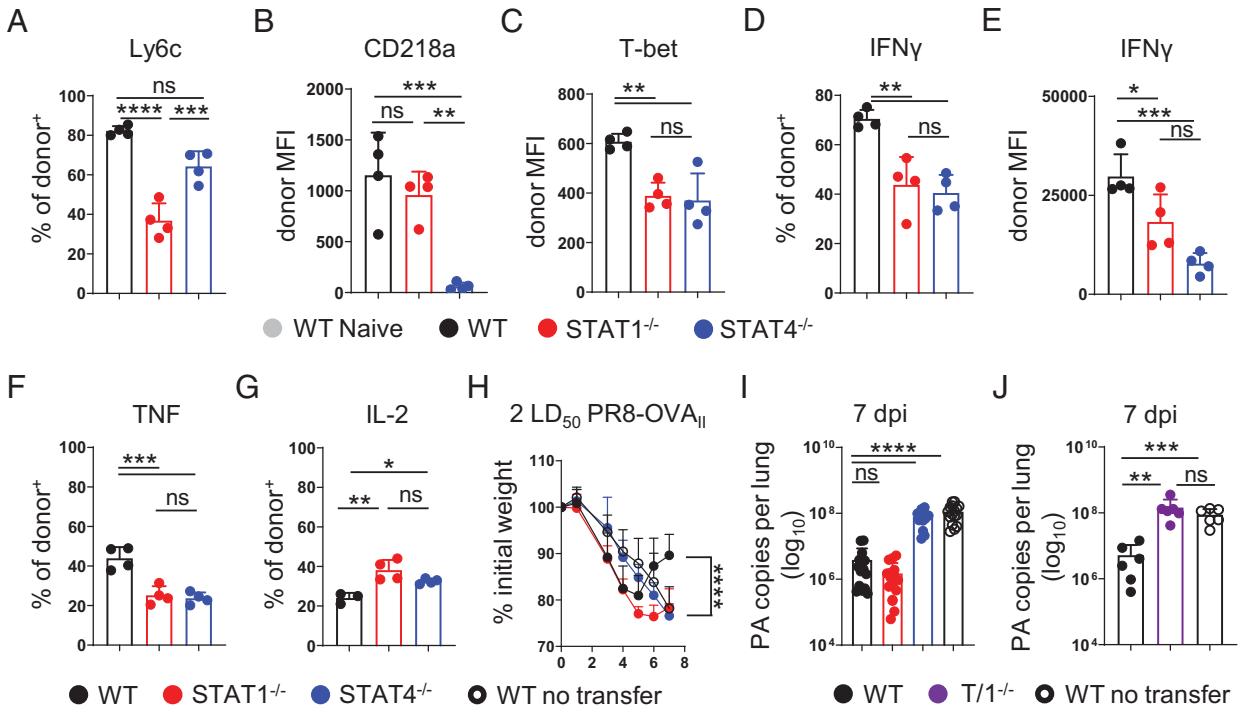

FIGURE 7. STAT4 activation enhances the protective capacity of Th1-primed effector cells against IAV. WT, $STAT1^{-/-}$, or $STAT4^{-/-}$ OT-II cells were cultured in Th1 conditions as in Figs. 1 and 3. The resulting effector cells (3×10^6) were transferred to unprimed congenic WT mice that were depleted of NK cells and then challenged with 2 LD_{50} of PR8-OVA_{II}. At 4 dpi, donors in the lungs of individual mice were analyzed for (**A**) $Ly6C^{high}$ cells, and the MFI of (**B**) CD218a and (**C**) T-bet, with (**D**) the frequency and (**E**) the MFI of IFN-γ^+ cells, and the frequency of (**F**) TNF^+, and (**G**) IL-2^+ cells. Results are from one of two experiments. Mice receiving WT, $STAT1^{-/-}$, or $STAT4^{-/-}$ effectors primed in Th1 conditions, or control mice not receiving cell transfer, were analyzed for (**H**) weight loss and recovery through 7 dpi and (**I**) pulmonary viral copies at 7 dpi. Results are for 16 mice per group; summary of two individual experiments. (**J**) NK cell–depleted mice receiving no transfer, or 3×10^6 WT, or $T/S1^{-/-}$ effectors primed in Th1 conditions were analyzed for viral copies at 7 dpi with 2 LD_{50} PR8-OVA_{II} (six mice per group; one of two experiments). $*p < 0.05$, $**p < 0.005$, $***p < 0.001$, $****p < 0.0001$. All error bars represent SD.

We next assessed the ability of the transferred effectors to protect the unprimed mice against IAV-induced disease by assessing weight loss kinetics as well as viral control at 7 dpi. WT effectors promoted recovery of weight loss compared with mice not receiving cells and mice receiving $STAT4^{-/-}$ effectors, both of which continued to lose weight through 7 dpi (Fig. 7H). Recipients of $STAT1^{-/-}$ cells lost more weight than WT recipients, but they did begin to recover, albeit 1 or 2 d later than WT recipients, resulting in significantly less weight recovery by $STAT1^{-/-}$ versus WT recipients at 7 dpi (Fig. 7H). Furthermore, mice receiving WT but not $STAT4^{-/-}$ cells controlled viral copies by over one log versus mice not receiving effector cells (Fig. 7I). Interestingly, despite differences in weight loss, viral control in $STAT1^{-/-}$ recipients was similar to that mediated by WT effectors (Fig. 7I).

Finally, we asked the extent to which the antiviral impact of the Th1-primed $STAT1^{-/-}$ effector cells is dependent on T-bet. In experiments transferring Th1-primed WT or $T/S1^{-/-}$ effectors to WT hosts, weight loss kinetics (not shown) and pulmonary viral copies detected at 7 dpi were similar in $T/S1^{-/-}$ recipients relative to mice not receiving cells, whereas WT effectors again promoted robust protection highlighted by significant viral control (Fig. 7J). STAT4 activation during priming in the absence of T-bet expression thus cannot promote effective antiviral CD4 T cell responses. Together, our findings indicate that protection provided by Th1 effectors against IAV is T-bet dependent and maximal when both STAT1 and STAT4 are engaged during priming.

Discussion

The mechanisms governing canonical Th subset polarization have been primarily defined in controlled in vitro settings. Overlaying these rules onto responses against pathogens in vivo has revealed important caveats and novel modes of regulation impacting not only CD4 T cell function but also their capacity to protect against disease. Here, we show that CD4 T cell–intrinsic STAT4 does not impact the phenotypic or functional Th1 attributes that mark WT cells primed by IAV, an infection often cited as an exemplar of inducing a strong Th1 response. In contrast, STAT1 is required to promote effectors expressing Th1 hallmarks at WT levels and, more important, to prevent the deletion of virus-activated CD4 T cells by NK cells. NK cell activity induced by IAV infection is greatest in the lungs (43, 44). This is in line with the near-total ablation of $STAT1^{-/-}$ cells in the lungs of mice with an intact NK cell compartment, with more $STAT1^{-/-}$ cells found in dLN and spleen. The full set of signals sensitizing $STAT1^{-/-}$ CD4 T cells to NK cell killing is unclear, but it is important to elucidate, given this mechanism's potential to impact disease outcomes (45). Decreased expression of MHC-I and Qa-2 have been correlated with predisposing CD4 T cells to NK cell attack in a noninfectious in vivo model (28), and we found expression of both to be reduced on $STAT1^{-/-}$ versus WT cells responding to IAV. We also speculate that increased IL-2 production by $STAT1^{-/-}$ versus WT CD4 T cells may contribute to their enhanced susceptibility to NK cell killing by promoting local NK cell activation (29). Defining the mechanisms by which NK cells eliminate the $STAT1^{-/-}$ effectors in our study also requires further investigation. However, we previously showed that several NK cell receptors redundantly, and to some extent collaboratively, promote CD4 T cell killing in cocultures of in vitro generated WT Th-polarized effectors and NK cells from lymphocytic choriomeningitis virus–infected mice (46). We also note that because we observed robust endogenous antiviral CD4 T cell responses in $STAT1^{-/-}$ mice, STAT1 activation in NK cells

appears to be critical in promoting their ability to kill IAV-primed CD4 T cells.

We found that the production of Th1-associated cytokines is compromised more severely in STAT1$^{-/-}$ than in T-bet$^{-/-}$ cells responding to IAV. Our in vivo and in vitro data indicate that some elements of STAT1-dependent control of effector function are thus independent from its role in promoting T-bet induction. A clear example of this is that IL-10 production, which is largely restricted to IFN-γ^{+} cells during IAV infection (33), is STAT1 but not T-bet dependent. Nevertheless, ~25% of IAV-primed T/S1$^{-/-}$ effector cells are still capable of IFN-γ production. We showed recently that IFN-γ production by T-bet$^{-/-}$ CD4 T cells is Eomes dependent (14). In vitro, Eomes expression is maximal in Th1-primed cells and significantly reduced in cells primed with IFN-γ or IL-12 alone, indicating synergy between STAT1 and STAT4 in inducing its expression. IL-12 treatment of IAV-infected mice also boosted Eomes expression by CD4 T cells in a STAT4-dependent manner, consistent with this pattern. However, IAV-primed STAT1$^{-/-}$ and T/S1$^{-/-}$ cells both expressed more Eomes than did T-bet$^{-/-}$ cells, which are themselves marked by higher levels of Eomes compared with WT cells. Indeed, regulation of Eomes by several mechanisms outside of the STAT1–STAT4–T-bet axis have been described (15), and our findings here suggest that such pathways may gain prominence when T-bet expression in CD4 T cell effectors is low or absent. We tried to generate STAT1$^{-/-}$/STAT4$^{-/-}$ double-knockout mice to further investigate this possibility but were unsuccessful. This may be due to the tight linkage of STAT1 and STAT4 on mouse chromosome 1 (47). An alternative means of eliminating STAT1 and STAT4 expression within the same CD4 T cell, perhaps through CRISPR or a similar approach, is thus required.

Higher CD127 expression on T-bet$^{-/-}$ cells correlates with their ability to outcompete WT cells with the same TcR specificity to form memory following IAV clearance (13). Our data here suggest that STAT1 engagement may promote memory fitness in T-bet$^{-/-}$ effectors because STAT1$^{-/-}$ and T/S1$^{-/-}$ effectors expressed less CD127 than T-bet$^{-/-}$ cells. However, we found that other markers implicated in memory fate, such as Ly6C (48), and TCF1 (49) (not shown), were not impacted by STAT1 deficincy in T-bet$^{-/-}$ cells. Further experiments are thus required to determine the extent to which circulating and lung-resident memory generation, which can be maintained in the absence of IL-7 (50), is impacted by the STAT1 pathway in CD4 T cells during IAV infection.

STAT1 activation is linked with the suppression of Th17 development in mice and humans in a variety of settings (51–56). A major mechanism by which STAT1 acts in this regard is by promoting the expression of T-bet in response to STAT1-dependent pro-Th1 cytokines such as IFN-γ. Indeed, WT cells primed by IAV that express relatively high levels of T-bet do not develop a strong Th17 component, whereas a sizable Th17 cohort does develop in T-bet$^{-/-}$ CD4 T cells in response to IL-6 and TGF-β signals in the infected lung (13, 14). It is thus surprising that we found a requirement for STAT1 expression by IAV-primed T-bet$^{-/-}$ CD4 T cells to promote Rorγt and hallmark Th17 functionality. However, blocking type I IFN signaling in IAV-infected mice restored Th17 responses by STAT1$^{-/-}$ cells that were similar in magnitude to those of T-bet$^{-/-}$ cells. On the basis of previous studies with CD8 T cells (38, 39) and the in vitro data presented here, type I IFN appears to act as a pro-Th1 factor during IAV infection in the absence of CD4 T cell–intrinsic STAT1 by signaling through STAT4. This in turn promotes expression of T-bet, Eomes, and IFN-γ and the concomitant repression of Th17 programming. This mechanism at first glance seems incompatible with the easily detectable Th17 cells in full STAT1$^{-/-}$ mice infected with IAV (25). However, the IAV-induced inflammatory environment in STAT1$^{-/-}$ mice is likely sufficiently altered from that in WT mice to nullify the requirement for STAT1 expression to enable Th17 polarization. This position is supported by our finding that even WT OT-II cells produce IL-17 in IAV-infected STAT1$^{-/-}$ but not STAT4$^{-/-}$ or WT hosts. That viral control in WT and STAT1$^{-/-}$ mice was similar in these experiments is also perhaps unexpected, given STAT1's key role in type I and type III signaling and the antiviral impacts of these pathways reported in many murine IAV studies (57). However, similar IAV titers in WT and STAT1$^{-/-}$ mice have been reported previously (25, 58), suggesting that type I and/or type III IFNs may signal through a noncanonical STAT1-independent pathway (59) in the STAT1$^{-/-}$ mice to promote efficient IAV control. In contrast to the critical role for STAT1 expression by CD4 T cells in promoting Th17 responses, STAT4 did not impact Th17 functionality in T-bet$^{-/-}$ CD4 T cells responding to IAV, despite its association with Th17 development in some studies. This fits our findings that Th17 development during IAV infection requires IL-6 and TGF-β (14) and that STAT4 seems to promote IL-23-dependent, but not IL-6/TGF-β-dependent, Th17 programing (60).

The broad similarities between WT and STAT4$^{-/-}$ CD4 T cell responses against IAV are surprising because, in contrast to some viruses such as lymphocytic choriomeningitis virus that do not induce robust IL-12 (61), IAV induces IL-12 at levels that are sufficient to impact elements of innate immune defense (62, 63). We postulate that IAV-induced IL-12 may be segregated physically or temporally from microenvironments where virus-specific CD4 T cells are primed. Indeed, macrophages appear to be a major producer of IL-12 during IAV infection (64), whereas its production is not detected from IAV-infected dendritic cells (65), which are the major APC involved in T cell priming. However, by treating IAV-primed mice with exogenous IL-12, we show that multiple aspects of Th1 identity can be enhanced through CD4 T cell–intrinsic STAT4 activation and that this boost is ultimately T-bet dependent. We speculate that the "weak" Th1 imprint induced in WT cells may underlie at least some aspects of the remarkable heterogeneity seen within the bulk IAV-primed CD4 T cell effector populations during both primary and recall responses (11, 66).

Our findings of improved protection mediated by effector cells with stronger versus weaker Th1 identity generated by engaging both STAT1 and STAT4 during priming agree with patterns found analyzing memory CD4 T cell–mediated protection against IAV. For example, we found previously that the transfer of Th1-polarized memory cells protected naive mice from lethal infection, whereas Th0 memory cells, which adopt weaker Th1 attributes in vivo, were less effective (67). Similarly, Farber and colleagues found that although the transfer of lung-retentive memory cells from IAV-primed mice protected naive mice against a lethal IAV challenge, an equal number of memory cells isolated from the spleen could not (68). The lung-derived cells in this study were marked by enhanced IFN-γ and reduced IL-2 production versus the splenic cells (68), matching the cytokine production patterns correlating with maximal protection provided by WT versus STAT1$^{-/-}$ and especially STAT4$^{-/-}$ effector cells primed in Th1 conditions. This supports the concept that vaccine strategies incorporating IL-12, or IL-12-inducing adjuvants, to boost Th1 polarization may improve CD4 T cell immunity and that this pathway supporting Th1 induction is not redundant with that initiated by STAT1 activation. Further studies are required to determine those STAT4-dependent genes induced by IL-12 that promote improved protective capacity. One potential mechanism is the IL-12-mediated upregulation of IL-18 receptor, because IL-18 has been shown to enhance cytokine production by mucosal-associated invariant T cells (69) and CD8 T cells responding to IAV (70). Vaccines targeting STAT4 activation in CD4 T cells may be particularly relevant to neonates and the aged that are marked by increased susceptibility to IAV and by weaker T cell

responses. Indeed, murine studies suggest that IL-12 signals can improve vaccine efficacy in these groups, though the underlying mechanisms have not been defined (71, 72).

In summary, we show that CD4 T cell–intrinsic STAT1 is needed for the Th1 hallmarks expressed by WT CD4 T cells primed by IAV and to prevent their deletion by NK cells. Unexpectedly, STAT1 is also required to promote Th17 responses against IAV that develop in the absence of CD4 T cell–intrinsic T-bet expression and that are highly protective in their own right (14, 33). In contrast, although it is crucial in directing canonical Th1 polarization in vitro, we find that the STAT4 pathway plays a minimal role in promoting antiviral CD4 T cell responses. Our findings are consistent with recent work indicating that the STAT4-dependent activation module is more prominently engaged during phagosomal versus viral infections (73). However, we show that STAT4 activation in IAV-primed CD4 T cells maximizes their Th1 imprint and promotes a robust T-bet-dependent antiviral effector program that STAT1 activation in the absence of STAT4 engagement cannot. This indicates that STAT1 and STAT4 are nonredundant in terms of promoting effective "Th1" cells in the setting of IAV infection. Our findings thus stress that care should be taken when characterizing responses as Th1, based on the presence of Th1 attributes and relative absence of those defining other subsets. Instead, they highlight important gradations in Th1 identity that can help to predict the ability of CD4 T cells to combat viruses and that can be modulated to improve outcomes.

Acknowledgments

We thank the University of Central Florida Lake Nona Vivarium staff for excellent care of the mice used in these studies and the University of Central Florida flow cytometry core facility. The graphical abstract was created with BioRender.com.

Disclosures

The authors have no financial conflicts of interest.

References

1. Swain, S. L., K. K. McKinstry, and T. M. Strutt. 2012. Expanding roles for CD4$^+$ T cells in immunity to viruses. *Nat. Rev. Immunol.* 12: 136–148.
2. Sant, A. J., K. A. Richards, and J. Nayak. 2018. Distinct and complementary roles of CD4 T cells in protective immunity to influenza virus. *Curr. Opin. Immunol.* 53: 13–21.
3. Belz, G. T., D. Wodarz, G. Diaz, M. A. Nowak, and P. C. Doherty. 2002. Compromised influenza virus-specific CD8$^+$-T-cell memory in CD4$^+$-T-cell-deficient mice. *J. Virol.* 76: 12388–12393.
4. Eichelberger, M., W. Allan, M. Zijlstra, R. Jaenisch, and P. C. Doherty. 1991. Clearance of influenza virus respiratory infection in mice lacking class I major histocompatibility complex-restricted CD8$^+$ T cells. *J. Exp. Med.* 174: 875–880.
5. Brown, D. M., S. Lee, M. L. Garcia-Hernandez, and S. L. Swain. 2012. Multifunctional CD4 cells expressing gamma interferon and perforin mediate protection against lethal influenza virus infection. *J. Virol.* 86: 6792–6803.
6. Strutt, T. M., K. K. McKinstry, Y. Kuang, L. M. Bradley, and S. L. Swain. 2012. Memory CD4$^+$ T-cell-mediated protection depends on secondary effectors that are distinct from and superior to primary effectors. *Proc. Natl. Acad. Sci. USA* 109: E2551–E2560.
7. Jansen, J. M., T. Gerlach, H. Elbahesh, G. F. Rimmelzwaan, and G. Saletti. 2019. Influenza virus-specific CD4$^+$ and CD8$^+$ T cell-mediated immunity induced by infection and vaccination. *J. Clin. Virol.* 119: 44–52.
8. McKinstry, K. K., R. W. Dutton, S. L. Swain, and T. M. Strutt. 2013. Memory CD4 T cell-mediated immunity against influenza A virus: more than a little helpful. *Arch. Immunol. Ther. Exp. (Warsz.)* 61: 341–353.
9. Wilkinson, T. M., C. K. Li, C. S. Chui, A. K. Huang, M. Perkins, J. C. Liebner, R. Lambkin-Williams, A. Gilbert, J. Oxford, B. Nicholas, et al. 2012. Preexisting influenza-specific CD4$^+$ T cells correlate with disease protection against influenza challenge in humans. *Nat. Med.* 18: 274–280.
10. Ruterbusch, M., K. B. Pruner, L. Shehata, and M. Pepper. 2020. In vivo CD4$^+$ T cell differentiation and function: revisiting the Th1/Th2 paradigm. *Annu. Rev. Immunol.* 38: 705–725.
11. Strutt, T. M., K. K. McKinstry, N. B. Marshall, A. M. Vong, R. W. Dutton, and S. L. Swain. 2013. Multipronged CD4$^+$ T-cell effector and memory responses cooperate to provide potent immunity against respiratory virus. *Immunol. Rev.* 255: 149–164.
12. Swain, S. L., J. N. Agrewala, D. M. Brown, D. M. Jelley-Gibbs, S. Golech, G. Huston, S. C. Jones, C. Kamperschroer, W. H. Lee, K. K. McKinstry, et al. 2006. CD4$^+$ T-cell memory: generation and multi-faceted roles for CD4$^+$ T cells in protective immunity to influenza. *Immunol. Rev.* 211: 8–22.
13. Dhume, K., C. M. Finn, T. M. Strutt, S. Sell, and K. K. McKinstry. 2019. T-bet optimizes CD4 T-cell responses against influenza through CXCR3-dependent lung trafficking but not functional programming. *Mucosal Immunol.* 12: 1220–1230.
14. Dhume, K., C. M. Finn, P. Devarajan, A. Singh, J. D. Tejero, E. Prokop, T. M. Strutt, S. Sell, S. L. Swain, and K. K. McKinstry. 2022. Bona fide Th17 cells without Th1 functional plasticity protect against influenza. *J. Immunol.* 208: 1998–2007.
15. Dhume, K., B. Kaye, and K. K. McKinstry. 2022. Regulation of CD4 T cell responses by the transcription factor eomesodermin. *Biomolecules* 12: 1549.
16. Pritchard, G. H., R. M. Kedl, and C. A. Hunter. 2019. The evolving role of T-bet in resistance to infection. *Nat. Rev. Immunol.* 19: 398–410.
17. Zhu, J., D. Jankovic, A. J. Oler, G. Wei, S. Sharma, G. Hu, L. Guo, R. Yagi, H. Yamane, G. Punkosdy, et al. 2012. The transcription factor T-bet is induced by multiple pathways and prevents an endogenous Th2 cell program during Th1 cell responses. *Immunity* 37: 660–673.
18. Furuta, S., S. Kagami, T. Tamachi, K. Ikeda, M. Fujiwara, A. Suto, K. Hirose, N. Watanabe, Y. Saito, I. Iwamoto, and H. Nakajima. 2008. Overlapping and distinct roles of STAT4 and T-bet in the regulation of T cell differentiation and allergic airway inflammation. *J. Immunol.* 180: 6656–6662.
19. Thieu, V. T., Q. Yu, H. C. Chang, N. Yeh, E. T. Nguyen, S. Sehra, and M. H. Kaplan. 2008. Signal transducer and activator of transcription 4 is required for the transcription factor T-bet to promote T helper 1 cell-fate determination. *Immunity* 29: 679–690.
20. Usui, T., R. Nishikomori, A. Kitani, and W. Strober. 2003. GATA-3 suppresses Th1 development by downregulation of Stat4 and not through effects on IL-12Rbeta2 chain or T-bet. *Immunity* 18: 415–428.
21. McKinstry, K. K., S. Golech, W. H. Lee, G. Huston, N. P. Weng, and S. L. Swain. 2007. Rapid default transition of CD4 T cell effectors to functional memory cells. *J. Exp. Med.* 204: 2199–2211.
22. Strutt, T. M., K. K. McKinstry, J. P. Dibble, C. Winchell, Y. Kuang, J. D. Curtis, G. Huston, R. W. Dutton, and S. L. Swain. 2010. Memory CD4$^+$ T cells induce innate responses independently of pathogen. *Nat. Med.* 16: 558–564.
23. Berenson, L. S., J. D. Farrar, T. L. Murphy, and K. M. Murphy. 2004. Frontline: absence of functional STAT4 activation despite detectable tyrosine phosphorylation induced by murine IFN-alpha. *Eur. J. Immunol.* 34: 2365–2374.
24. Hwang, E. S., J. H. Hong, and L. H. Glimcher. 2005. IL-2 production in developing Th1 cells is regulated by heterodimerization of RelA and T-bet and requires T-bet serine residue 508. *J. Exp. Med.* 202: 1289–1300.
25. Lee, B., R. Gopal, M. L. Manni, K. J. McHugh, S. Mandalapu, K. M. Robinson, and J. F. Alcorn. 2017. STAT1 is required for suppression of type 17 immunity during influenza and bacterial superinfection. *Immunohorizons* 1: 81–91.
26. Bot, A., E. Rodrigo, T. Wolfe, S. Bot, and M. G. Von Herrath. 2003. Infection-triggered regulatory mechanisms override the role of STAT 4 in control of the immune response to influenza virus antigens. *J. Virol.* 77: 5794–5800.
27. Thomas, P. G., S. A. Brown, W. Yue, J. So, R. J. Webby, and P. C. Doherty. 2006. An unexpected antibody response to an engineered influenza virus modifies CD8$^+$ T cell responses. *Proc. Natl. Acad. Sci. USA* 103: 2764–2769.
28. Kang, Y. H., A. Biswas, M. Field, and S. B. Snapper. 2019. STAT1 signaling shields T cells from NK cell-mediated cytotoxicity. *Nat. Commun.* 10: 912.
29. Arbelaez, C. A., P. Palle, J. Charaix, and E. Bettelli. 2022. STAT1 signaling protects self-reactive T cells from control by innate cells during neuroinflammation. *JCI Insight* 7: e148222.
30. McKinstry, K. K., F. Alam, V. Flores-Malavet, M. Z. Nagy, S. Sell, A. M. Cooper, S. L. Swain, and T. M. Strutt. 2019. Memory CD4 T cell-derived IL-2 synergizes with viral infection to exacerbate lung inflammation. *PLoS Pathog.* 15: e1007989.
31. McKinstry, K. K., T. M. Strutt, B. Bautista, W. Zhang, Y. Kuang, A. M. Cooper, and S. L. Swain. 2014. Effector CD4 T-cell transition to memory requires late cognate interactions that induce autocrine IL-2. *Nat. Commun.* 5: 5377.
32. Swain, S. L., M. C. Jones, P. Devarajan, J. Xia, R. W. Dutton, T. M. Strutt, and K. K. McKinstry. 2021. Durable CD4 T-cell memory generation depends on persistence of high levels of infection at an effector checkpoint that determines multiple fates. *Cold Spring Harb. Perspect. Biol.* 13: a038182.
33. McKinstry, K. K., T. M. Strutt, A. Buck, J. D. Curtis, J. P. Dibble, G. Huston, M. Tighe, H. Hamada, S. Sell, R. W. Dutton, and S. L. Swain. 2009. IL-10 deficiency unleashes an influenza-specific Th17 response and enhances survival against high-dose challenge. *J. Immunol.* 182: 7353–7363.
34. Lazarevic, V., X. Chen, J. H. Shim, E. S. Hwang, E. Jang, A. N. Bolm, M. Oukka, V. K. Kuchroo, and L. H. Glimcher. 2011. T-bet represses T_H17 differentiation by preventing Runx1-mediated activation of the gene encoding RORγt. *Nat. Immunol.* 12: 96–104.
35. Peters, A., K. D. Fowler, F. Chalmin, D. Merkler, V. K. Kuchroo, and C. Pot. 2015. IL-27 induces Th17 differentiation in the absence of STAT1 signaling. *J. Immunol.* 195: 4144–4153.
36. Meyer Zu Horste, G., D. Przybylski, M. A. Schramm, C. Wang, A. Schnell, Y. Lee, R. Sobel, A. Regev, and V. K. Kuchroo. 2018. Fas promotes T helper 17 cell differentiation and inhibits T helper 1 cell development by binding and sequestering transcription factor STAT1. *Immunity* 48: 556–569.e7.
37. Villarino, A. V., E. Gallo, and A. K. Abbas. 2010. STAT1-activating cytokines limit Th17 responses through both T-bet-dependent and -independent mechanisms. *J. Immunol.* 185: 6461–6471.

38. Nguyen, K. B., W. T. Watford, R. Salomon, S. R. Hofmann, G. C. Pien, A. Morinobu, M. Gadina, J. J. O'Shea, and C. A. Biron. 2002. Critical role for STAT4 activation by type 1 interferons in the interferon-gamma response to viral infection. *Science* 297: 2063–2066.
39. Gil, M. P., M. J. Ploquin, W. T. Watford, S. H. Lee, K. Kim, X. Wang, Y. Kanno, J. J. O'Shea, and C. A. Biron. 2012. Regulating type 1 IFN effects in CD8 T cells during viral infections: changing STAT4 and STAT1 expression for function. *Blood* 120: 3718–3728.
40. Nakahira, M., M. Tomura, M. Iwasaki, H. J. Ahn, Y. Bian, T. Hamaoka, T. Ohta, M. Kurimoto, and H. Fujiwara. 2001. An absolute requirement for STAT4 and a role for IFN-gamma as an amplifying factor in IL-12 induction of the functional IL-18 receptor complex. *J. Immunol.* 167: 1306–1312.
41. Morris, S. C., K. B. Madden, J. J. Adamovicz, W. C. Gause, B. R. Hubbard, M. K. Gately, and F. D. Finkelman. 1994. Effects of IL-12 on in vivo cytokine gene expression and Ig isotype selection. *J. Immunol.* 152: 1047–1056.
42. Brown, D. M., A. M. Dilzer, D. L. Meents, and S. L. Swain. 2006. CD4 T cell-mediated protection from lethal influenza: perforin and antibody-mediated mechanisms give a one-two punch. *J. Immunol.* 177: 2888–2898.
43. Carlin, L. E., E. A. Hemann, Z. R. Zacharias, J. W. Heusel, and K. L. Legge. 2018. Natural killer cell recruitment to the lung during influenza A virus infection is dependent on CXCR3, CCR5, and virus exposure dose. *Front. Immunol.* 9: 781.
44. Stegemann-Koniszewski, S., S. Behrens, J. D. Boehme, I. Hochnadel, P. Riese, C. A. Guzmán, A. Kröger, J. Schreiber, M. Gunzer, and D. Bruder. 2018. Respiratory influenza A virus infection triggers local and systemic natural killer cell activation via Toll-like receptor 7. *Front. Immunol.* 9: 245.
45. Waggoner, S. N., M. Cornberg, L. K. Selin, and R. M. Welsh. 2011. Natural killer cells act as rheostats modulating antiviral T cells. *Nature* 481: 394–398.
46. Daniels, K. A., C. L. O'Donnell, C. Castonguay, T. M. Strutt, K. K. McKinstry, S. L. Swain, and R. M. Welsh. 2020. Virus-induced natural killer cell lysis of T cell subsets. *Virology* 539: 26–37.
47. Copeland, N. G., D. J. Gilbert, C. Schindler, Z. Zhong, Z. Wen, J. E. Darnell, Jr., A. L. Mui, A. Miyajima, F. W. Quelle, J. N. Ihle, et al. 1995. Distribution of the mammalian Stat gene family in mouse chromosomes. *Genomics* 29: 225–228.
48. Marshall, H. D., A. Chandele, Y. W. Jung, H. Meng, A. C. Poholek, I. A. Parish, R. Rutishauser, W. Cui, S. H. Kleinstein, J. Craft, and S. M. Kaech. 2011. Differential expression of Ly6C and T-bet distinguish effector and memory Th1 $CD4^+$ cell properties during viral infection. *Immunity* 35: 633–646.
49. Nish, S. A., K. D. Zens, R. Kratchmarov, W. W. Lin, W. C. Adams, Y. H. Chen, B. Yen, N. J. Rothman, A. Bhandoola, H. H. Xue, et al. 2017. $CD4^+$ T cell effector commitment coupled to self-renewal by asymmetric cell divisions. *J. Exp. Med.* 214: 39–47.
50. Strutt, T. M., K. Dhume, C. M. Finn, J. H. Hwang, C. Castonguay, S. L. Swain, and K. K. McKinstry. 2018. IL-15 supports the generation of protective lung-resident memory CD4 T cells. *Mucosal Immunol.* 11: 668–680.
51. Liu, L., S. Okada, X. F. Kong, A. Y. Kreins, S. Cypowyj, A. Abhyankar, J. Toubiana, Y. Itan, M. Audry, P. Nitschke, et al. 2011. Gain-of-function human STAT1 mutations impair IL-17 immunity and underlie chronic mucocutaneous candidiasis. *J. Exp. Med.* 208: 1635–1648.
52. Puel, A. 2020. Human inborn errors of immunity underlying superficial or invasive candidiasis. *Hum. Genet.* 139: 1011–1022.
53. Feng, G., W. Gao, T. B. Strom, M. Oukka, R. S. Francis, K. J. Wood, and A. Bushell. 2008. Exogenous IFN-gamma ex vivo shapes the alloreactive T-cell repertoire by inhibition of Th17 responses and generation of functional $Foxp3^+$ regulatory T cells. *Eur. J. Immunol.* 38: 2512–2527.
54. Kulkarni, M. M., S. Varikuti, C. Terrazas, J. L. Kimble, A. R. Satoskar, and B. S. McGwire. 2015. Signal transducer and activator of transcription 1 (STAT-1) plays a critical role in control of *Trypanosoma cruzi* infection. *Immunology* 145: 225–231.
55. Leon-Cabrera, S., A. Vázquez-Sandoval, E. Molina-Guzman, Y. Delgado-Ramirez, N. L. Delgado-Buenrostro, B. E. Callejas, Y. I. Chirino, C. Pérez-Plasencia, M. Rodríguez-Sosa, J. E. Olguín, et al. 2018. Deficiency in STAT1 signaling predisposes gut inflammation and prompts colorectal cancer development. *Cancers (Basel)* 10: 341.
56. Marié, I. J., L. Brambilla, D. Azzouz, Z. Chen, G. V. Baracho, A. Arnett, H. S. Li, W. Liu, L. Cimmino, P. Chattopadhyay, et al. 2021. Tonic interferon restricts pathogenic IL-17-driven inflammatory disease via balancing the microbiome. *eLife* 10: e68371.
57. Wu, W., and J. P. Metcalf. 2020. The role of type I IFNs in influenza: antiviral superheroes or immunopathogenic villains? *J. Innate Immun.* 12: 437–447.
58. García-Sastre, A., R. K. Durbin, H. Zheng, P. Palese, R. Gertner, D. E. Levy, and J. E. Durbin. 1998. The role of interferon in influenza virus tissue tropism. *J. Virol.* 72: 8550–8558.
59. Stanifer, M. L., K. Pervolaraki, and S. Boulant. 2019. Differential regulation of type I and type III interferon signaling. *Int. J. Mol. Sci.* 20: 1445.
60. Mathur, A. N., H. C. Chang, D. G. Zisoulis, G. L. Stritesky, Q. Yu, J. T. O'Malley, R. Kapur, D. E. Levy, G. S. Kansas, and M. H. Kaplan. 2007. Stat3 and Stat4 direct development of IL-17-secreting Th cells. *J. Immunol.* 178: 4901–4907.
61. Dalod, M., T. P. Salazar-Mather, L. Malmgaard, C. Lewis, C. Asselin-Paturel, F. Brière, G. Trinchieri, and C. A. Biron. 2002. Interferon alpha/beta and interleukin 12 responses to viral infections: pathways regulating dendritic cell cytokine expression in vivo. *J. Exp. Med.* 195: 517–528.
62. Monteiro, J. M., C. Harvey, and G. Trinchieri. 1998. Role of interleukin-12 in primary influenza virus infection. *J. Virol.* 72: 4825–4831.
63. Hwang, I., J. M. Scott, T. Kakarla, D. M. Duriancik, S. Choi, C. Cho, T. Lee, H. Park, A. R. French, E. Beli, et al. 2012. Activation mechanisms of natural killer cells during influenza virus infection. *PLoS One* 7: e51858.
64. Hama, Y., M. Kurokawa, M. Imakita, Y. Yoshida, T. Shimizu, W. Watanabe, and K. Shiraki. 2009. Interleukin 12 is a primary cytokine responding to influenza virus infection in the respiratory tract of mice. *Acta Virol.* 53: 233–240.
65. Bhardwaj, N., R. A. Seder, A. Reddy, and M. V. Feldman. 1996. IL-12 in conjunction with dendritic cells enhances antiviral $CD8^+$ CTL responses in vitro. *J. Clin. Invest.* 98: 715–722.
66. Strutt, T. M., K. K. McKinstry, and S. L. Swain. 2009. Functionally diverse subsets in CD4 T cell responses against influenza. *J. Clin. Immunol.* 29: 145–150.
67. McKinstry, K. K., T. M. Strutt, Y. Kuang, D. M. Brown, S. Sell, R. W. Dutton, and S. L. Swain. 2012. Memory $CD4^+$ T cells protect against influenza through multiple synergizing mechanisms. *J. Clin. Invest.* 122: 2847–2856.
68. Teijaro, J. R., D. Turner, Q. Pham, E. J. Wherry, L. Lefrançois, and D. L. Farber. 2011. Cutting edge: Tissue-retentive lung memory CD4 T cells mediate optimal protection to respiratory virus infection. *J. Immunol.* 187: 5510–5514.
69. Loh, L., Z. Wang, S. Sant, M. Koutsakos, S. Jegaskanda, A. J. Corbett, L. Liu, D. P. Fairlie, J. Crowe, J. Rossjohn, et al. 2016. Human mucosal-associated invariant T cells contribute to antiviral influenza immunity via IL-18-dependent activation. *Proc. Natl. Acad. Sci. USA* 113: 10133–10138.
70. Denton, A. E., P. C. Doherty, S. J. Turner, and N. L. La Gruta. 2007. IL-18, but not IL-12, is required for optimal cytokine production by influenza virus-specific $CD8^+$ T cells. *Eur. J. Immunol.* 37: 368–375.
71. Arulanandam, B. P., J. N. Mittler, W. T. Lee, M. O'Toole, and D. W. Metzger. 2000. Neonatal administration of IL-12 enhances the protective efficacy of antiviral vaccines. *J. Immunol.* 164: 3698–3704.
72. Khan, T., C. L. Heffron, K. P. High, and P. C. Roberts. 2014. Tailored vaccines targeting the elderly using whole inactivated influenza vaccines bearing cytokine immunomodulators. *J. Interferon Cytokine Res.* 34: 129–139.
73. Krueger, P. D., M. F. Goldberg, S. W. Hong, K. C. Osum, R. A. Langlois, D. I. Kotov, T. Dileepan, and M. K. Jenkins. 2021. Two sequential activation modules control the differentiation of protective T helper-1 (Th1) cells. *Immunity* 54: 687–701.e4.